Industrial Automation and Intra-Household Labor Supply

Claudio Costanzo*

January 23, 2026

Abstract

Industrial automation disproportionately displaces male-dominated routine tasks, raising women's potential wages relative to men's. Combining American Time Use Survey (ATUS) data with a shift-share measure of local robot exposure, I document a reallocation of household time going against wage incentives: greater exposure leads women to withdraw from the market and increase time in childcare and leisure, while men increase market hours. The effect tends to be amplified in areas with historically high share of religious attendance, suggesting that these patterns are driven by gender identity norms. To quantify this friction, I estimate a structural household model with a "breadwinner" identity wedge. The model replicates non-monotonicity in time use observed in the data and implies that identity norms double the gender gap in market hours relative to a neutral benchmark.

Keywords: Childcare; Gender identity norms; Household labor supply; Industrial automation; Relative wages.

JEL Codes: J16, J22, J31, D13, O33, F16.

*ECARES, Université Libre de Bruxelles. Contact: claudio.costanzo@ulb.be

1 Introduction

Over the last few decades, industrial automation has fundamentally reshaped the labor market landscape in advanced economies. The diffusion of industrial robots disproportionately displaces routine, brawn-intensive tasks—traditionally performed by men—while simultaneously increasing the relative demand for cognitive and interpersonal tasks, areas where women typically possess the advantage (de Vries et al., 2020). Consequently, this technological adoption functions as a gender-equalizing force, narrowing the gender wage gap by devaluing male-dominated routine labor (Ge and Zhou, 2020; Giuntella et al., 2024), and decreasing the marriage market value of men (Anelli et al., 2021). Figure 1 plots the distribution of occupational robot exposure by sex.[1] Occupations at the upper end of the distribution (i.e., those with high automation risk) are predominantly male, whereas those at the lower end are predominantly female.

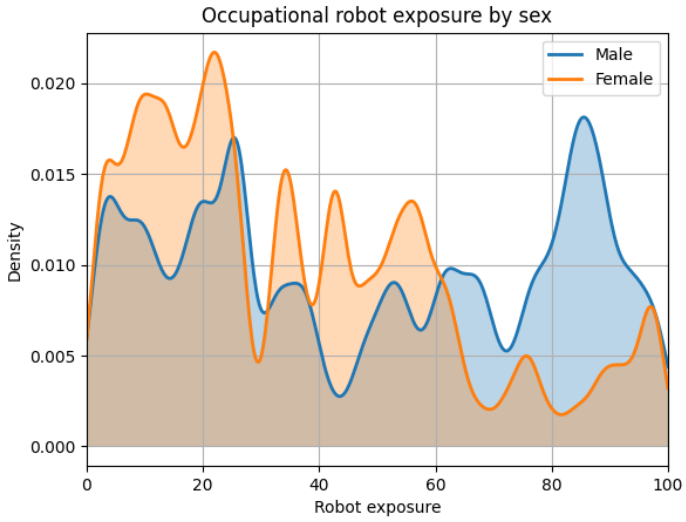

Figure 1: Kernel densities of robot exposure by sex. Source: United States IPUMS Census/ACS microdata, 2000–2020 (Flood et al., 2024). The figure displays the distribution of the robot-exposure score constructed by Webb (2019).

This study traces the consequences of these structural shifts for intra-household time allocation, focusing on how automation, by raising women's relative wages, reshapes the balance between market labor and household production.

Standard neoclassical theories of household labor supply, such as the unitary or collective models with Pareto-efficient allocations, predict a clear response to such shifts: as a spouse's

[1] Webb (2019) constructs robot exposure by measuring the textual overlap between O*NET task descriptions and robot-related patent text. This measurement strategy reflects a fundamental distinction: robot exposure is task-based—determined by an occupation's task mix.

relative wage and productivity rise, that spouse should substitute time away from home production and toward market work (Becker, 1965; Chiappori, 1992). Within this framework, industrial automation should theoretically "unlock" female labor supply by increasing the opportunity cost of home production.

In this paper, I document a behavioral pattern that challenges this standard prediction. By linking the American Time Use Survey (ATUS) to local labor market exposure to industrial robots, I find that greater exposure—and the associated rise in women's relative wages—induces women to reallocate time away from the market and toward home production and leisure. Specifically, for every standard deviation increase in robot exposure, women reduce market work in favor of leisure and childcare by approximately one hour per day. Conversely, men in exposed households increase their market hours.

In commuting zones with a high share of traditional religious adherents (e.g., Southern Baptist, Mormon), women's withdrawal from the labor market is nearly three times larger than in less conservative areas, suggesting that social norms regarding family specialization drive this effect. "Breadwinner" norms impose a psychological or social penalty on couples when the wife's earnings approach or surpass those of her husband (Bertrand et al., 2015). Because robot-induced shocks disproportionately depress male earnings in the lower-middle segment of the distribution, they push a significant mass of households toward earnings parity—the threshold where identity norms are most likely to bind.

To address endogeneity concerns inherent in shift-share measures, I instrument U.S. industry-level robot adoption with contemporaneous adoption trends in five European economies: Denmark, Finland, France, Italy, and Sweden. This strategy isolates variation in relative wages driven by global technological frontiers, orthogonal to local labor market conditions or regional gender attitudes. The results remain robust to controlling for concurrent trade shocks (the "China shock"), adjusting for sample selection into marriage, and accounting for the correlation in residuals across areas that have similar sectoral compositions.

To quantify the economic magnitude of these norms, I develop and estimate a structural, semi-cooperative household model of time allocation. A penalty term—defined as a function of the wife's earnings relative to the husband's—captures the disutility arising from violations of the breadwinner norm. I estimate the model parameters using the Simulated Method of Moments (SMM) to match the non-monotonic time-use profiles observed in the ATUS. The structural estimates reveal that identity norms approximately double the gender gap in market hours relative to an identity-neutral benchmark.

Counterfactual analyses simulating automation-induced shocks to men's wages highlight three findings: (i) the norm induces a kink at the equal-earnings threshold, generating an inverse-U shape in women's market hours (with a mirror pattern in childcare); (ii) aggregate

effects scale nonlinearly with the distribution of relative wages, as shifts moving couples beyond parity disproportionately increase the share of households for which the norm binds; and (iii) the norm depresses welfare relative to the efficient benchmark by reallocating time away from market work, even when wives possess high market productivity.

The paper makes four distinct contributions to the literature. First, it examines how industrial automation reshapes family dynamics. While Anelli et al. (2021) document that automation reduces marriage rates due to a decline in men's marriage-market value, and Matysiak et al. (2023); Costanzo (2025) link it to fertility choices, this study focuses on the intensive margin: how automation alters spouses' joint decision-making regarding the allocation of time between market and non-market activities.

Second, by exploiting variation in spouses' relative potential wages induced by industrial robots, I address methodological concerns regarding the "identity norm" hypothesis (Bertrand et al., 2015). Literature suggests that apparent behavioral anomalies at the point of earnings parity may stem from misreporting (Heggeness and Murray-Close, 2019; Rosenberg, 2021) or endogenous labor supply convergence (Zinovyeva and Tverdostup, 2021). By utilizing industrial automation as an exogenous source of wage variation, The paper isolate the causal link between relative earnings and time allocation, circumventing the endogeneity of reported earnings.

Third, I develop and estimate a structural household time-use model that reproduces the observed non-monotonic relationship between time allocation and spouses' wage shares. Unlike prior structural models focusing on general wage shocks (Blundell et al., 2018) or parental education (Gobbi, 2018), this framework explicitly captures how shifts in relative wage shares—specifically those driven by automation—reshape the trade-offs between market work, childcare, and leisure.

Finally, the paper bridges the disconnect between micro and macro labor supply elasticities by highlighting the role of social norms. While standard macro theory predicts smooth household insurance responses like the "added worker effect" (Stephens Jr., 2001), empirical evidence documents significant optimization frictions (Chetty et al., 2011; Bick and Fuchs-Schündeln, 2018). The model identifies identity norms as a structural friction that explains this divergence, showing why households fail to reallocate labor efficiently when the husband's status is threatened.

The remainder of the paper is organized as follows. Section 2 describes the data, sample restrictions, and the construction of the instrumented shift-share robot exposure. Section 3 details the empirical specification and presents OLS, 2SLS, and robustness results. Section 4 documents stylized facts (Section 4.1) before developing and estimating the structural model. Section 5 concludes.

2 Data, sample, and measurement

The main data for the analysis are gathered from the American Time Use Survey (ATUS) and the International Federation of Robotics (IFR).

Time use. The ATUS provides nationally representative, diary-based measures of minutes spent on activities over a 24-hour day. The survey has run continuously since 2003, drawing one respondent (age 15+) from households that recently completed the CPS. The analysis sample consists of married or cohabiting households with at least one employed spouse and at least one child aged 10 or younger (following Blundell et al., 2018). Market work corresponds to the ATUS category "work and work-related activities." Childcare time is measured by aggregating "Caring for and helping household children," "Activities related to household children's education," and "Activities related to household children's health."

Table 1 presents summary statistics for the primary analysis sample—married or cohabiting households with young children—while Appendix Table A1 provides a comparison with the general ATUS population. The presence of children aged ten or younger marks a significant shift in time-use priorities, characterized by a substantial reallocation of time from leisure toward childcare and market work.

For men in the analysis sample, daily leisure averages 262 minutes, a sharp decline from the 357 minutes observed in the general population. This "leisure deficit" is largely absorbed by a heightened commitment to the labor market; men in the sample record 261.95 minutes of market work per day (compared to 191 minutes generally) and report usual weekly hours of 44.0, significantly above the 30.9-hour average for the broader male population.

Women's time-use profiles reveal a different set of trade-offs. While their market work time remains relatively stable (132 minutes/day in the sample vs. 127 minutes in the general population), they experience a more severe compression of leisure, which falls from 310 to 226.80 minutes per day. This reduction is primarily driven by the intensive demands of childcare, which averages 142.94 minutes per day for women in the sample—nearly double the 79.19 minutes recorded by their male partners. The analysis sample is younger and more highly educated than the general population, with over 44% of both men and women holding tertiary degrees.

Industrial robots. Data on the operational stock of industrial robots at the country–year–sector level are sourced from the International Federation of Robotics (IFR). The IFR compiles these data through annual surveys of robot suppliers, covering the period from 1993 to 2019. Following the ISO 8373:2012 standard, the IFR defines an industrial robot as an "automatically controlled, reprogrammable, multipurpose manipulator, programmable in

Table 1: Descriptive statistics: ATUS analysis sample (households with young children)

	Females			Males		
Variable	Obs	Mean	Std. Dev.	Obs	Mean	Std. Dev.
Leisure (min/day)	24,748	226.80	164.97	22,021	262.00	195.74
Childcare (min/day)	24,748	142.94	147.38	22,021	79.19	113.27
Market work (min/day)	24,748	132.19	215.60	22,021	261.95	277.40
Age	24,748	35.49	6.78	22,021	38.05	7.54
Hourly wage (USD)	7,381	16.45	10.49	7,839	18.68	10.21
Weekly earnings (USD)	14,013	757.96	534.22	16,666	1,086.80	594.43
Usual work hours per week	23,048	23.56	19.61	20,463	44.00	14.24
Less than secondary (%)	24,748	7.85	26.90	22,021	8.72	28.22
Secondary (%)	24,748	19.12	39.33	22,021	22.17	41.54
Some college (%)	24,748	26.54	44.16	22,021	24.83	43.20
Tertiary (%)	24,748	46.48	49.88	22,021	44.28	49.67

Notes: The sample is restricted to married/cohabiting households with at least one employed spouse and at least one child aged $\leq$10. Leisure, childcare, and market work are ATUS diary minutes/day. Hourly wage, weekly earnings, and usual hours are derived from the linked CPS files. Education rows report the share (%) within each attainment category.

three or more axes." Crucially, these machines are fully autonomous and do not require a dedicated human operator to perform their tasks, distinguishing them from simpler forms of automated machinery or software-based ICT capital.

The trajectory of robot adoption in the United States is illustrated in Figure 2. While the initial diffusion of industrial robotics began to rise notably in the early 1990s, the pace of adoption accelerated sharply after the turn of the millennium, reflecting a fundamental shift in the technological frontier of American manufacturing.

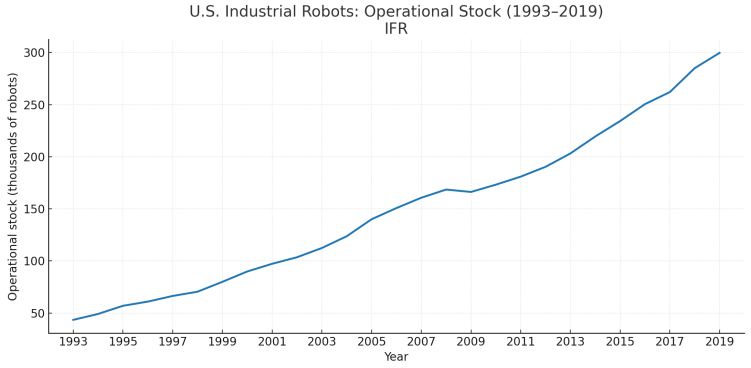

Figure 2: U.S. industrial robot operational stock, 1993–2019 (IFR).

Despite its comprehensive coverage, the IFR dataset presents specific measurement challenges. Sectoral disaggregation for the U.S. is consistently available only starting in 2004. To

maintain a high degree of granularity, the analysis leverages detailed data for 13 manufacturing sub-sectors and six non-manufacturing categories.[2] For robots not classified by industry in the original data, I follow the standard literature by allocating them proportionally based on the classified distribution within the country. Finally, because the IFR provides data only at the national level, local labor market exposure must be constructed using the industrial composition of commuting zones, as detailed in the following section.

2.1 Local exposure to robots

The explanatory variable measures local labor market exposure to industrial robotics at the commuting-zone level using a Bartik-style instrument, following Acemoglu and Restrepo (2020). This approach assumes a uniform distribution of robots across industries within a commuting zone, exploiting variation in the pre-sample local employment distribution by sector and the national evolution of robot stocks.

In line with standard shift-share measures, the variable is anchored to the industrial composition of local labor markets before the surge in industrial automation. By using historical differences in regional industrial specialization, this approach addresses endogeneity concerns arising from the possibility that current employment levels are influenced by the same unobserved factors driving robot adoption. Historical specialization is proxied by the 1990 employment share in the commuting zone, retrieved from Census data. The measure of exposure in a given industry is obtained by multiplying the baseline local employment share by the national ratio of robots to employed workers.[3] Subsequently, the industry-specific scores are summed to obtain the commuting-zone exposure to industrial robotics:

$$Robots_{ct} = \sum_{s} \frac{Emp_{sc}^{90}}{Emp_{c}^{90}} \times \frac{StockRobots_{st}}{Emp_{s}^{90}}, \tag{1}$$

where subscripts s, c, and t denote industry, commuting zone, and year, respectively. Emp_{sc}^{90} represents the number of employed workers in industry s and commuting zone c in 1990, and Emp_{c}^{90} is total employment in the commuting zone. The term $\frac{StockRobots_{st}}{Emp_{s}^{90}}$ denotes the number of robots per thousand workers relative to the 1990 baseline.

Endogeneity concerns may arise from several sources. For instance, local labor markets with stronger employment protection legislation may face higher labor costs, incentivizing

[2]The categories are: Agriculture and Fishery, Automotive, Construction, Electronics, Food and Beverages, Furniture, Basic Metals, Machinery, Metal Products, Non-metallic Minerals, Mining, Paper, Petrochemicals, Research, Services, Textiles, Utilities, and Non-automotive Vehicles.

[3]Approximately one-third of industrial robots are not classified by sector; these are allocated proportionally based on the classified data, as in Acemoglu and Restrepo (2020).

firms to install more robots. While this is mitigated by including state-year fixed effects (as laws are typically enacted at the state level), other local factors—such as union strength or labor supply responses to economic conditions correlated with automation—could still bias the estimates.

To address these issues, I instrument U.S. robot adoption using robot usage in European economies. The instrument is defined as:

$$Robots_{ct}^{IV} = \frac{1}{5} \sum_{j \in \text{EU5}} \left(\sum_{s} \frac{Emp_{sc}^{70}}{Emp_{c}^{70}} \times \frac{StockRobots_{st}^{j}}{Emp_{s}^{j,90}} \right), \tag{2}$$

where $j \in$ EU5 refers to Denmark, Finland, France, Italy, and Sweden. These countries are ahead of the U.S. in robot adoption.[4] The instrument interacts the historical industrial specialization of the labor market in 1970 (to avoid mechanical correlation with pre-1990 U.S. robot adoption) with the penetration of robots per thousand workers in European country j. The 1990 employment levels for the five European countries are retrieved from EUKLEMS (van Ark and Jäger, 2017).

This instrument exploits common industry-specific trends in automation driven by global technological supply shocks rather than local U.S. demand. Since the global automation trend is driven by a small number of international robot suppliers, the relevance of $Robots_{ct}^{IV}$ is theoretically well-founded. Validity requires that European industry-level automation affects U.S. time use only via its impact on U.S. robot adoption—i.e., not through concurrent global industry shocks, trade linkages, or macro conditions, conditional on controls and fixed effects.

Table 2 reports summary statistics for the shift-share measure. Robot exposure has a mean of 3.22 (SD 4.12); by construction, one unit corresponds approximately to one additional robot per 1,000 workers.

Table 2: Summary statistics of robot shift-share measure.

Variable	**Mean**	**Std. Dev.**	**Min.**	**Max.**	**N**
Robots	3.218	4.122	0.816	33.704	80,635

[4]Germany, while a leader in automation, is excluded from the instrument because its adoption rates are far higher than other countries and may follow different structural patterns than the U.S. or the EU5.

3 The effect of robots on time use

This section describes the pooled cross-section model used to examine the relationship between exposure to automation and household time use choices. It then presents the 2SLS results and robustness checks.[5]

3.1 Empirical model

The baseline specification is:

$$Y_{ict} = \alpha + \beta \, \text{Robots}_{ct} + \eta' C_{ict} + \gamma_c + \delta_{s(c)\times t} + \varepsilon_{ict}, \tag{3}$$

where Y_{ict} represents minutes/day in market work, leisure, and childcare spent by individual i; Robots_{ct} is the shift–share measure for commuting zone c in year t; and C_{ict} includes temporal, demographic, and economic controls (day of week, month, holiday; number of children; respondent's and spouse's age and education; indicators for children under 5; ages of youngest and oldest child; and family–income category). γ_c are commuting-zone fixed effects and $\delta_{s(c)\times t}$ are state-by-year fixed effects. β represents the change in Y_{ict} for one additional robot per 1,000 workers. Regressions use ATUS survey weights, and standard errors are clustered at the commuting-zone–year level. Active job seekers (unemployed and looking for a job) are excluded to reduce bias driven by the direct unemployment effects of the shocks.

To address endogeneity, I estimate two-stage least squares (2SLS), instrumenting Robots_{ct} with its external shifter:

$$\text{Robots}_{ct} \;=\; \pi \, \text{Robots}^{IV}_{ct} + \eta' C_{ict} + \gamma_c + \delta_{s(c)\times t} + u_{ct}, \tag{4}$$

which yields the fitted value $\widehat{\text{Robots}}_{ct}$. The second stage replaces the endogenous regressor with this fitted value:

$$Y_{ict} = \alpha + \beta \, \widehat{\text{Robots}}_{ct} + \eta' C_{ict} + \gamma_c + \delta_{s(c)\times t} + \varepsilon_{ict}. \tag{5}$$

3.2 Results

This section reports estimation results on three subsamples defined by spouses' employment: households in which the spouse of the respondent works, households in which the respon-

[5] Throughout the 2SLS analyses, the Kleibergen and Paap (2006) F-statistics hover around a value of 300, indicating strong first-stage relevance.

dent works, and households in which both spouses work. This setup allows me to consider both intensive and extensive margins in time allocation. In all specifications, Robots_{ct} is instrumented with the corresponding external shifter (EU5 industry robot adoption).

Table 3 shows the response of daily time use to a one-unit increase in robot exposure (roughly one additional robot per 1,000 workers). For men, market work rises significantly: by approximately 14 minutes when including corner solutions (column 1), by roughly 8 minutes for respondent-employed individuals (column 2), and by 18 minutes in two-earner households (column 3). Simultaneously, men's leisure falls by roughly 12 minutes in two-earner households.

For women, the patterns are reversed. Market work declines by approximately 15 minutes per day in the full sample (column 4) and by roughly 19 minutes when conditioning on employment (column 5). This time is reallocated primarily toward home production: childcare time rises by about 6 to 8 minutes (columns 4–6), and leisure increases by 7 to 11 minutes. Given the exposure standard deviation of about 4, a one-standard-deviation increase scales these per-unit effects by roughly four, implying substantial shifts in daily routines.

Overall, robot exposure drives a distinct reallocation of time within couples: women shift out of market work into childcare and leisure, while men shift into market work (and out of leisure), with effects particularly pronounced in households where both spouses are employed.

3.3 Mechanism: The Role of Traditional Family Norms

The results presented above pose a challenge to standard theories of household labor supply. Since industrial robots primarily displace brawn-intensive tasks—traditionally a male comparative advantage—automation theoretically tilts the terms of trade within the household in favor of women. In a frictionless collective model, this shift in comparative advantage should induce households to reallocate time toward female market work. Moreover, to the extent that automation depresses male earnings, the resulting negative income shock should trigger an "added worker effect," prompting women to increase labor supply to smooth household consumption (Stephens Jr., 2002). The data, however, reveal the opposite pattern: a contraction in women's market hours despite their improving relative market position.

These dynamics can arise from family identity norms. Exposure to automation disproportionately compresses men's earnings in the lower-middle of the distribution, pushing a significant mass of couples toward the earnings parity threshold where breadwinner norms bind (Bertrand et al., 2015). In this region, the psychological cost of the wife out-earning her husband acts as a high marginal tax rate on her labor, effectively suppressing the incentive to

Table 3: Effect of robots on time spent working, childcaring, and leisuring per day (2SLS Estimates).

	Males			Females		
	(1)	(2)	(3)	(4)	(5)	(6)
Daily minutes work						
Robots	13.92**	8.376*	18.02**	-15.40***	-18.76***	-15.26**
	(6.598)	(4.618)	(7.384)	(5.073)	(5.899)	(6.628)
Observations	6,795	6,582	3,905	7,668	4,974	4,546
R-squared	0.426	0.455	0.529	0.297	0.430	0.476
Daily minutes childcare						
Robots	0.160	1.687	-0.773	5.579*	8.220***	8.455**
	(2.533)	(2.111)	(2.707)	(2.975)	(2.701)	(3.383)
Observations	6,795	6,582	3,905	7,668	4,974	4,546
R-squared	0.170	0.179	0.323	0.230	0.232	0.290
Daily minutes leisure						
Robots	-4.019	-3.869	-11.87***	7.214**	10.13***	10.67***
	(3.400)	(3.365)	(3.818)	(2.968)	(3.186)	(3.918)
Observations	6,795	6,582	3,905	7,668	4,974	4,546
R-squared	0.251	0.262	0.362	0.215	0.310	0.353
Spouse employed	✓		✓	✓		✓
Respondent employed		✓	✓		✓	✓

Notes: Sample includes married or cohabiting couples with at least one spouse working and children aged 10 or less. Control variables in all specifications include state-by-year fixed effects, spouses' age and education, number of children (total and under age 5), ages of the youngest and oldest child, day-of-week and month-of-survey fixed effects, and a holiday indicator. Standard errors clustered at the commuting-zone–year level are in parentheses. *** $p < 0.01$, ** $p < 0.05$, * $p < 0.1$.

work. Consequently, households forgo consumption smoothing to preserve traditional gender roles, resulting in the observed withdrawal of women from the market and the compensatory increase in male work hours.

To test this mechanism directly, I exploit spatial variation in cultural attitudes toward gender roles rooted in religious affiliation. I construct a measure of "traditional norms" using data from the *Churches and Church Membership in the United States, 1990* dataset, collected by the Association of Statisticians of American Religious Bodies (ASARB). I use the 1990 baseline—prior to the main wave of robot adoption—to ensure that local religious composition is not endogenous to contemporaneous economic shocks.

Following the literature linking conservative religious affiliation to traditional gender attitudes (Glass and Nath, 2006; Guiso et al., 2003), I calculate the share of the population in each county belonging to denominations that emphasize traditional family structures and male breadwinning. The set of denominations includes the Church of Jesus Christ of Latter-day Saints (Mormons), the Southern Baptist Convention, the Assemblies of God, the Lutheran Church–Missouri Synod, and the Presbyterian Church in America, among others. I aggregate these adherent counts to the Commuting Zone (CZ) level using the crosswalk provided by Autor and Dorn (2013) and divide by the total CZ population to obtain the local share of traditional adherents.

I define a binary indicator D_c^{High} equal to one if a commuting zone's share of traditional adherents is above the sample median. I then estimate an augmented specification that interacts robot exposure with this indicator:

$$Y_{ict} = \alpha + \beta_1 \text{Robots}_{ct} + \beta_2 (\text{Robots}_{ct} \times D_c^{High}) + \eta' C_{ict} + \gamma_c + \delta_{s(c)\times t} + \varepsilon_{ict}. \tag{6}$$

In this framework, β_1 captures the baseline effect of automation in socially progressive regions, while β_2 captures the *additional* impact in socially conservative regions. Both terms are instrumented using the corresponding interactions of the European robot instrument.

Table 4 presents the results. For men (Columns 1–3), the interaction term is statistically insignificant across all specifications for market work. This null result is economically revealing: it suggests that male labor supply responses to automation are driven primarily by economic necessity (the income effect from falling wages) rather than cultural constraints. Men in progressive and conservative areas face the same economic shock and respond identically by attempting to increase market hours.

In sharp contrast, the results for women (Columns 4–6) reveal striking heterogeneity. In progressive commuting zones (the baseline group), an additional robot per 1,000 workers reduces women's market work by approximately 14 minutes per day (Column 6). However, in

conservative commuting zones, this negative effect is significantly amplified. The interaction term indicates an additional withdrawal of roughly 26 minutes per day ($p < 0.10$), implying a total reduction of approximately 40 minutes per day in high-norm areas. This total effect is nearly triple the magnitude found in progressive regions.

The asymmetry of these results—null for men, strong for women—provides compelling evidence for the identity mechanism. While economic shocks drive the male response uniformly across regions, the female response is heavily conditioned by the local cultural environment. In communities where the "breadwinner" norm is most salient, the identity cost effectively forces women to withdraw from the labor market, overriding the consumption-smoothing motives that would otherwise prevail.

An alternative explanation is that these shocks operate through a purely technological channel: labor-saving innovations may reduce the number of worker-minutes required to produce a given level of output. Under this mechanism, one would expect to see shorter market hours and offsetting increases in leisure even among individuals without a co-resident partner, since the change in time requirements would be independent of household structure. Appendix Table A2 provides evidence against this interpretation. For individuals not in a relationship, the estimated effects on market, childcare and leisure time are close to zero, suggesting that the main results are not driven by generalized reductions in the time intensity of work tasks but rather by intra-household responses to relative earnings shifts.

3.4 Industrial Automation vs. Trade Shocks

As an additional exercise, I compare the effects of industrial automation with those of rising import competition from China. The literature has established that the "China shock" had profound effects on U.S. labor markets, particularly by depressing manufacturing employment and wages for men (Autor et al., 2013). Furthermore, similar to the robot shock, trade-induced manufacturing decline has been shown to degrade the "marriage-market value" of young men, leading to lower marriage and fertility rates (Autor et al., 2019). Figure 3 confirms that men are disproportionately concentrated in occupations with high exposure to tradable goods industries.[6]

Despite these similarities, trade and automation operate on the household budget con-

[6]The tradable share is computed as the pooled, person-weighted probability for each occupation o that a worker i is employed in a tradable industry:

$$\hat{p}_o = \frac{\sum_{i \in o} w_i \, \mathbf{1}\{\text{Industry}_i \in T\}}{\sum_{i \in o} w_i},$$

where T includes Agriculture/Forestry/Fishing, Mining, Manufacturing, Transport/Communications/Utilities, and Wholesale Trade.

Table 4: Heterogeneity by Local Gender Norms (IV Estimates)

	Males			Females		
	(1)	(2)	(3)	(4)	(5)	(6)
Daily minutes market work						
Trad × Robots	-5.888	7.377	-2.769	-31.11**	-24.35**	-25.85*
	(15.98)	(14.27)	(15.85)	(12.59)	(11.77)	(15.59)
Robots	12.74**	7.989**	14.01**	-13.16***	-16.74***	-14.41**
	(5.755)	(3.935)	(6.191)	(4.756)	(5.397)	(5.998)
Observations	4,506	7,306	4,193	7,967	5,400	4,844
R-squared	0.425	0.441	0.477	0.280	0.421	0.430
Daily minutes childcare						
Trad × Robots	5.178	5.730	0.275	19.42**	4.414	-0.176
	(7.328)	(6.103)	(6.883)	(8.603)	(5.580)	(7.253)
Robots	0.496	2.588	1.419	3.075	8.957***	9.350***
	(2.280)	(2.007)	(2.235)	(2.546)	(2.837)	(3.019)
Observations	4,506	7,306	4,193	7,967	5,400	4,844
R-squared	0.224	0.172	0.246	0.236	0.227	0.241
Daily minutes leisure						
Trad × Robots	-12.72	-11.96	-5.996	6.486	14.36*	21.04*
	(11.39)	(8.519)	(10.76)	(7.169)	(8.718)	(11.01)
Robots	-5.545	-3.493	-8.995***	6.066**	10.22***	8.534**
	(3.830)	(3.116)	(3.196)	(3.031)	(2.918)	(3.482)
Observations	4,506	7,306	4,193	7,967	5,400	4,844
R-squared	0.288	0.256	0.311	0.206	0.300	0.310
Spouse employed	✓		✓	✓		✓
Respondent employed		✓	✓		✓	✓

Notes: The table reports 2SLS estimates of the effect of robot exposure interacted with local gender norms. "Trad" is a binary indicator equal to one if the commuting zone has an above-median share of adherents to traditional religious denominations in 1990. Sample: married or cohabiting couples with at least one spouse working and children aged 10 or less. Control variables in all specifications include state-by-year fixed effects, spouses' age and education, number of children (total and under age 5), ages of the youngest and oldest child, day-of-week and month-of-survey fixed effects, and a holiday indicator. Standard errors clustered at the commuting-zone–year level are in parentheses. *** $p < 0.01$, ** $p < 0.05$, * $p < 0.1$.

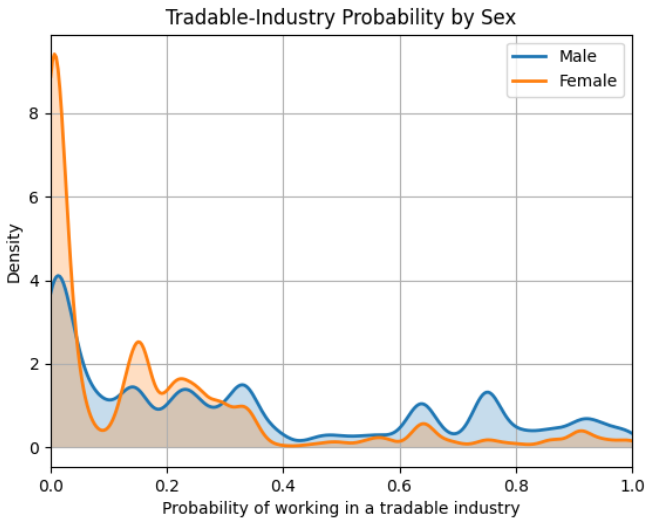

Figure 3: Kernel densities of tradable industry probability by sex. Source: United States IPUMS Census/ACS microdata, 2000–2020 (Flood et al., 2024).

straint through potentially conflicting margins. Trade shocks typically manifest as industry-level contractions involving extensive-margin adjustments, such as plant closures and permanent layoffs (Halla et al., 2020). This generates a theoretical ambiguity. On one hand, the loss of male income should trigger an "added worker effect," compelling wives to increase labor supply to smooth consumption (Besedeš et al., 2021). On the other hand, the degradation of male status might trigger the same identity-based withdrawal observed with automation.

In contrast, industrial robots represent a *task-based shock* that substitutes for human labor at the intensive margin, often allowing the firm to remain viable while devaluing male tasks (Acemoglu and Restrepo, 2020). Because automation depresses male potential wages without necessarily forcing immediate unemployment, the "added worker" motive may be less salient than the "identity" motive. By comparing these two shocks, I test whether the identity mechanism generalizes to trade: if trade shocks yield similar (albeit potentially weaker) estimates, it suggests that the identity norm is powerful enough to dampen or even override the added worker effect even in the context of manufacturing decline.

To isolate these channels, I perform two exercises. First, I replicate the baseline estimations replacing robot exposure with commuting-zone exposure to Chinese imports (Autor et al., 2013). Second, I perform a formal robustness check by re-estimating the primary robot-exposure coefficients while explicitly controlling for the trade shock. This ensures that the impact of automation on household labor supply is not an artifact of concurrent globalization trends.

Measurement of the trade shock. The data for this exercise are integrated from several sources. Detailed bilateral trade data by product and year are retrieved from the UN Comtrade Database. Domestic production and absorption values used to normalize the shocks are sourced from the U.S. Census Bureau and the NBER-CES Manufacturing Industry Database. Historical industry-specific employment at the commuting-zone level is derived from the Decennial Census/ACS microdata and County Business Patterns (CBP), following the regional definitions in Autor et al. (2013).

U.S. imports from China have expanded significantly since the early 1990s, driven by market reforms, large-scale rural-to-urban migration, and enhanced access to foreign technology and capital. These domestic transformations, together with China's accession to the WTO—which granted it permanent normal trade relations status—have markedly increased its export capacity. As shown in Figure 4, imports from China began rising in the 1990s, entered a phase of exponential growth starting with the 2001 WTO accession, and finally leveled off around 2014.[7]

Figure 4: U.S. goods imports from China, 1990–2024 (Census basis, nominal).

Following Autor et al. (2013), I extract annual bilateral export flows from China by product to the United States and to other high-income destinations. Product-level values are mapped to U.S. industries using standard NAICS concordances and aggregated to construct industry-level Chinese import exposure.

To construct the measure of local exposure to import competition, I employ the shift-share methodology of Autor et al. (2013). The shock captures the cumulative growth in Chinese import penetration within a commuting zone, weighted by the zone's historical industrial composition. Specifically, industry-level imports from China are mapped to 397 four-digit SIC manufacturing industries using NAICS-to-SIC concordances. The local exposure is

[7]Therefore, the ATUS sample used to investigate the effect of import competition is restricted to the period 2003–2014.

defined as:

$$\text{Trade}_{ct} = \sum_{s} \frac{Emp_{sc,90}}{Emp_{c,90}} \times \frac{\Delta\text{Import}_{st}^{Ch\to US}}{Absorption_{s,90}}, \tag{7}$$

where $\Delta\text{Import}_{st}^{Ch\to US} = \text{Import}_{st}^{Ch\to US} - \text{Import}_{s,91}^{Ch\to US}$ represents the growth in U.S. imports from China in industry s between the base year (1991) and year t. The denominator is the sector's 1990 domestic absorption (total production plus imports minus exports). I rely on the change in exposure relative to the baseline, rather than the contemporaneous level, to isolate the structural displacement shock affecting labor demand—analogous to the robot exposure measure—rather than capturing persistent regional differences in trade openness.[8]

To address the endogeneity of U.S. import penetration—specifically the concern that import growth might reflect U.S. domestic demand shocks rather than Chinese supply factors—I instrument U.S. exposure using industry-level growth of Chinese exports to eight other high-income countries (Australia, Denmark, Finland, Germany, Japan, New Zealand, Spain, and Switzerland). The instrument Trade_{ct}^{IV} replaces the U.S. import term with foreign import flows and uses 1980 employment shares as weights to mitigate mechanical correlations with contemporaneous labor market adjustments.

Gender-oriented decomposition. A key feature of the trade shock is its variation across sectors with differing gender intensities. While industrial automation is identified by task content, trade exposure can be decomposed to isolate shocks that load heavily on male-dominated versus female-dominated industries. This allows for a more direct comparison with the male-biased nature of robot adoption. Using the historical female share of employment in each industry-commuting zone pair, $f_{cs,90}$, and its complement, $1 - f_{cs,90}$, I decompose the overall exposure into gender-specific shocks:

$$\text{Trade}_{ct}^{g} = \sum_{s} s_{cs,90}^{g} \times \frac{Emp_{sc,90}}{Emp_{c,90}} \times \frac{\Delta\text{Import}_{st}^{Ch\to US}}{Absorption_{s,90}}, \quad g \in \{f, m\}, \tag{8}$$

where $s_{cs,90}^{f} = f_{cs,90}$ and $s_{cs,90}^{m} = 1 - f_{cs,90}$. This decomposition identifies two distinct sources of variation: Trade_{ct}^{m} targets sectors like heavy manufacturing and basic metals where men prevail, while Trade_{ct}^{f} loads on sectors like textiles and electronics with higher female employment shares.

Table 5 reports summary statistics for the aggregate and gender-specific trade measures. The aggregate exposure to Chinese import competition (Trade_{ct}) has a mean of 0.006 and

[8]Unlike the trade measure, the robot exposure variable defined in Equation 1 does not require explicit differencing from a base year. Since the operational stock of industrial robots in the early 1990s was negligible across most industries, the contemporaneous stock $StockRobots_{st}$ is effectively equivalent to the cumulative change in adoption since the beginning of the sample period.

a standard deviation of 0.010. Given the construction of the variable as a weighted average of industry-level import penetration ratios, a one-standard-deviation increase corresponds roughly to a 1 percentage point rise in the share of Chinese imports in domestic absorption.

Decomposing this exposure reveals the gendered nature of the shock. The male-specific component (Trade^m_{ct}), which isolates exposure in male-dominated industries, averages 0.003 (SD 0.005). In contrast, the female-specific component (Trade^f_{ct}) is smaller, with a mean of 0.002 (SD 0.004).

Table 5: Summary statistics of trade exposure measures.

Variable	Mean	Std. Dev.	Min.	Max.	N
Trade_{ct}	0.006	0.010	0	0.163	168,414
Trade^m_{ct}	0.003	0.005	0	0.059	168,414
Trade^f_{ct}	0.002	0.004	0	0.044	168,414

China shock results. Table A3 provides the first set of comparative results using the aggregate Chinese import penetration measure. In contrast to the robot exposure estimates, which often show a diverging response between spouses, rising import competition typically induces a simultaneous reduction in market hours for both partners on the intensive margin. Specifically, the 2SLS estimates for the two-earner sample (column 3 for men, column 6 for women) indicate that a 1 percentage point increase in import penetration reduces male market work by roughly 51 minutes per day and female market work by 29 minutes.

Despite the general contraction in market hours, the reallocation toward home production remains gendered: women significantly increase their time in childcare (by approximately 21 minutes per day in column 6), whereas the effect for men is smaller and lacks statistical precision. This suggests that while trade shocks act as a more generalized "negative wealth shock" that depresses labor supply across the board due to the extensive-margin loss of manufacturing jobs, the internal household response still defaults to women providing the bulk of compensatory childcare.

The decomposition into Trade_{Male} and Trade_{Fem} in Table A4 allows for a more granular test of the identity-norm mechanism. The Trade_{Male} shock serves as a specular benchmark for the robot analysis, as it disproportionately targets male-dominated manufacturing hubs, thereby raising the wife's relative wage share.

Under Trade_{Male}, we observe dynamics that largely mirror the automation results: men in two-earner households significantly reduce their leisure time (by approximately 147 to 176 minutes per 1 pp in 2SLS), consistent with an effort to maintain market attachment or

household contribution as their sector declines. In contrast, the results for Trade_{Fem}—which loads on sectors where women prevail—show a distinct reversal. Here, the shock to the wife's relative earnings leads to a large and significant withdrawal of the husband from market work (roughly 277 minutes per 1 pp) and an increase in his leisure.

Joint estimation of robot and trade shocks. As a final robustness check, I estimate a "horse-race" specification that includes both robot exposure and Chinese import competition simultaneously. This strategy allows me to isolate the impact of task-based automation while holding constant the broader effects of manufacturing decline and globalization. Table A5 presents the results.

For market work and leisure, the coefficients on robot exposure remain remarkably consistent with the baseline estimates, and in some cases, become even more pronounced. In the 2SLS specification for two-earner households (Column 3), the positive effect of robots on male market work nearly doubles to 36.37 minutes (compared to 18.02 in the baseline), suggesting that trade and automation may exert opposing pressures on male labor supply. Conversely, the negative effect on female market work remains stable in magnitude but varies in precision: it retains statistical significance in the broader sample of households (Column 4, coefficient -15.69^{*}), but loses significance at the intensive margin (Column 6), despite the point estimate remaining large (-16.63). Similarly, the reallocation of time toward leisure—a reduction for men and an increase for women—is preserved and remains statistically significant (Columns 3 and 6).

However, the results for childcare time are less robust in the joint estimation. While the baseline specification indicated a significant shift toward female childcare, the coefficients in Table A5 shrink in magnitude and become statistically insignificant for both spouses. This sensitivity suggests that the specific reallocation of non-market time toward childcare is difficult to disentangle from the broader disruptions caused by trade shocks, or that the high spatial correlation between the two shocks inflates standard errors. Nevertheless, the stability of the results for market work and leisure confirms that the core finding—automation shifting intra-household labor supply toward a traditional gendered allocation—is not an artifact of concurrent trade patterns.

3.5 Robustness

The following robustness checks address potential threats to identification and sample validity that may arise in the main specification.

Representativeness of the ATUS sample: The effect on wages. A potential concern in using the American Time Use Survey (ATUS) to study the impact of technology shocks is its relatively smaller sample size and specific coverage compared to the Decennial Census or the American Community Survey (ACS) typically used in the literature (e.g., Acemoglu and Restrepo (2020)). If the labor market effects of robotization estimated within the ATUS sample deviate significantly from established findings, it would imply that the main results on time allocation might be driven by sample selection specificities rather than general equilibrium adjustments.

To validate the representativeness of the sample, I estimate Commuting Zone (CZ) level wage regressions using aggregated ATUS microdata. I employ a stacked long-difference specification rather than the standard annual two-way fixed effects approach used in the main time-use analysis. This choice is motivated by two factors. First, consistent with the automation literature, local labor markets adjust to structural shocks over the medium-to-long run; annual wage data is often subject to transitory fluctuations and business cycle noise that can obscure the structural impact of robot adoption (Acemoglu and Restrepo, 2020). Second, the ATUS sample size is significantly smaller than that of the Census. When disaggregated to the CZ level, annual observations often yield cells with few respondents, leading to substantial measurement error. Using short-term differences would exacerbate attenuation bias due to high sampling error. Relying on stacked differences over 3, 5, and 7 years smooths out high-frequency sampling noise and isolates the structural variation necessary to identify the causal effects of the shocks.

The model is specified as follows:

$$\Delta \ln w_{ct} = \beta \cdot \Delta \text{Robots}_{ct} + \gamma' X_{c,1990} + \delta_t + \epsilon_{ct}, \tag{9}$$

where $\Delta \ln w_{ct}$ is the change in the average log hourly wage for men or women in commuting zone c over period t (3, 5, or 7 years). The term $\Delta \text{Robots}_{ct}$ represents the change in exposure to automation. The vector $X_{c,1990}$ includes the standard set of 1990 baseline controls: demographics, education levels, and manufacturing industry shares. All regressions are weighted by the ATUS population weights aggregated to the CZ level and include period fixed effects δ_t.

Table A6 reports the 2SLS results. In the short run (3-year difference, Columns 1–3), I observe a statistically significant and economically meaningful negative effect of robotization on male wages ($\beta = -0.061$, $p < 0.01$). This decline drives a significant narrowing of the gender wage gap ($\beta = -0.050$). Extending the analysis to 5- and 7-year differences, the negative impact on male wages remains robust and statistically significant, although the

magnitude of the coefficient attenuates over longer horizons (diminishing to -0.014 in the 7-year specification). Similarly, while the point estimates for the wage gap remain negative across all horizons, the effect is most precisely estimated in the short run.

Despite the inherent power limitations of the ATUS subsample, these estimates do not diverge from the patterns typically found using broader Census or ACS data. The results confirm that robot adoption exerts consistent downward pressure on the wages of the exposed group—men—validating the premise that the time-use shifts documented in the main analysis are responses to real labor market value erosion.

Correction for sample selection bias. A potential threat to the identification strategy arises from endogenous sample selection. Recent empirical evidence indicates that negative labor market shocks driven by automation significantly alter family formation dynamics. Anelli et al. (2021) document that the decline in men's marriage-market value in exposed regions reduces marriage rates, increases cohabitation, and elevates divorce risk. Consequently, limiting the analysis to married or cohabiting couples with young children may introduce bias if the shocks systematically alter the unobserved composition of households selected into the sample (e.g., if progressive dual-earner couples are more likely to dissolve or delay childbearing in response to the shock than traditional couples).

To address this concern, I implement an Inverse Probability Weighting (IPW) procedure to correct for selection into the analytical sample. I define the underlying "at-risk" population as all individuals in the ATUS aged 20–55, regardless of marital or parental status. I then estimate a probit model to predict the probability, $P(S_{ict} = 1)$, that an individual i in commuting zone c at time t satisfies the baseline sample inclusion criteria S (being married or cohabiting). The selection equation is specified as:

$$P(S_{ict} = 1 \mid \text{Robots}_{ct}^{IV}, \mathbf{X}_{ict}) = \Phi\left(\alpha + \gamma \text{Robots}_{ct}^{IV} + \mathbf{X}_{ict}'\beta + \delta_r\right), \tag{10}$$

where $\mathbf{X}_{ict}$ represents a vector of demographic controls (age, education, race) and δ_r denotes Census-region fixed effects. Crucially, I include the *external instrument* Robots_{ct}^{IV} (European robot adoption) rather than the endogenous exposure measure. Using the instrument in the selection equation ensures that the correction isolates selection driven by exogenous global technological trends, rather than by local unobservables (e.g., local management practices or plant closures) that might simultaneously affect adoption and household stability.

From the estimated parameters of Equation (10), I calculate the propensity score $\hat{p}_{ict}$ and construct inverse probability weights $w_{ict}^{IPW} = 1/\hat{p}_{ict}$. These weights up-weight observations that are statistically under-represented in the restricted sample relative to the general

population due to the global shocks. I then re-estimate the baseline 2SLS specifications (Equation 5), weighting observations by the product of the original ATUS survey weight and w_{ict}^{IPW}. By restoring the representativeness of the sample with respect to shock exposure, this procedure ensures that the estimates capture behavioral changes in time allocation rather than compositional shifts in the household population.

Table A7 presents the estimates corrected for sample selection. The results remain quantitatively robust to the IPW correction: the point estimates for market work and leisure are statistically indistinguishable from the baseline results, confirming that the observed reallocation of time is driven by intra-household adjustments rather than differential selection into marriage or parenthood.

Weekly hours worked. ATUS diaries capture a single day and feature many zero-work diaries (e.g., full-time workers sampled on a day off), which raises outcome noise and makes estimates sensitive to functional-form assumptions in the presence of corner solutions (Hamermesh et al., 2005; Stewart, 2013). To verify that the findings are not an artifact of this one-day snapshot, Table A8 re-estimates the baseline using respondents' "usual weekly hours" at their main job from the CPS interview that precedes the ATUS—a measure that averages over day-to-day variation and exhibits far fewer zeros. Because usual hours are collected for workers, these regressions condition on employment.

The coefficients remain tightly aligned with the diary-based estimates. For women, a one-unit increase in robot exposure reduces usual working time by approximately 1.0 to 1.3 hours per week (Columns 4–6). This magnitude is consistent with the daily reduction of roughly 15–18 minutes found in the diary estimates (Table 3), which translates to approximately 1.25 to 1.5 hours over a five-day workweek.

Accounting for the automotive industry. A common concern with shift-share measures of robot exposure, emphasized by Goldsmith-Pinkham et al. (2020), is that their variation may be driven by sector-specific trends, potentially undermining causal interpretation. The vehicle sector is especially problematic because the automotive industry has been the largest adopter of robots in the U.S.[9] Appendix Table A9 reports the Rotemberg weights used to construct the Bartik measure, confirming that the vehicle sector receives a disproportionately large weight compared to other industries.

To address this issue, Appendix Table A10 controls for commuting-zone-specific trends across quartiles of employment share in the vehicle sector. The coefficients remain broadly

[9]See Figure 2 in Acemoglu and Restrepo (2020) regarding the rapid rise in robot penetration in this sector relative to other industries in both the U.S. and European labor markets between 1993 and 2007.

consistent with the primary findings. While there is a slight decrease in statistical precision for women's market work at the intensive margin (Column 6, where the p-value exceeds conventional thresholds), the point estimates for both men and women across most specifications remain stable and economically significant.

Shock-based standard errors (AKM). To account for the correlation of errors across regions sharing similar industries, I apply the shift-share inference method proposed by Adão et al. (2019). Standard clustering at the commuting-zone level may understate standard errors if residuals are correlated through shared sectoral shocks. The AKM approach re-centers inference on the sectors (shocks) rather than the regions. I first residualize both the outcome and the shift-share regressor with respect to controls and fixed effects, then aggregate these residuals to the sector level using the exposure weights. The variance is computed based on the limit sequence where the number of sectors goes to infinity, allowing for arbitrary within-sector correlation.

Applying the AKM estimator of Adão et al. (2019) leaves the qualitative patterns intact, though precision is naturally more conservative (Table A11). For women, the reduction in market work remains highly statistically significant across all 2SLS specifications (Columns 4–6), as does the increase in leisure. For childcare, the intensive-margin effect in two-earner households remains robust and significant.

For men, the results are more sensitive to this conservative inference. While the increase in market work remains large and significant for two-earner households, the coefficients in the broader samples (Columns 1–2) are no longer statistically distinguishable from zero. Overall, the AKM inference confirms the core finding of a within-household reallocation: women significantly withdraw from market work in favor of leisure and childcare, while men in dual-earner households intensify their market hours.

The next section proposes a formalization of the causal intuition through a structural collective model of household time allocation, with parameters estimated by matching ATUS data on time use.

4 A structural household model of time use

Starting from showing stylized facts on nonlinearities between women wage shares and households' time use as a potential mechanism, this section elaborates a collective household model to reproduce the kink in time allocation and formalize the causal intuition of the empirical results. Individuals choose how much time to allocate to market work, leisure, and childcare in a model based on the semi-cooperative framework of Gobbi (2018).

4.1 Stylized facts on wage shares and time use

This section presents descriptive evidence on how relative wages shape household time allocation. When a woman's share of total household wages exceeds her partner's, both spouses reallocate their time between work, childcare, and leisure in distinct ways. Appendix Section B further shows that ISSP data reveal that this non-monotonic pattern extends to family-oriented beliefs. Finally, building on these stylized facts, the section explores a potential causal mechanism underlying the empirical patterns documented in Section 3.

Data from the ATUS are used to examine the relationship between spouses' wage shares and household time allocation. The sample is restricted to married or cohabiting couples under age 64 with at least one child aged ten or younger. Following Bertrand et al. (2015), hourly wages are calculated by dividing weekly earnings by weekly hours worked.[10] For non-workers, a potential wage is imputed as the mean wage of employed individuals sharing the same education level, five-year age bracket, state of residence, and survey year. Including non-workers allows for the consideration of adjustments on both the intensive and extensive margins of labor supply.

Figure 5 plots average daily minutes spent working, providing childcare, and engaging in leisure against the wife's wage share,[11] with separate linear trends fitted on either side of the parity point. The data reveal striking slope changes (kinks) around the equal-earnings threshold (0.5).

As the wife's wage share rises toward parity, her working time increases; however, upon crossing the threshold, the trend reverses, forming an inverse-V shape. Her childcare time mirrors this with a V-shaped pattern: it declines as her relative earnings rise toward parity, but reverts to an upward trend once she becomes the primary earner.

A corresponding reversal characterizes men's time use. Male market work exhibits a V-shape—decreasing as the wife contributes more, but rising sharply once she out-earns him. Conversely, male childcare and leisure follow an inverse-V pattern, increasing up to the parity point before declining. These patterns suggest that once the "breadwinner" hierarchy is threatened, households deviate from standard specialization models, with men increasing market effort and women compensating by taking on more non-market tasks.

4.2 Model set-up

The analysis relies on a semi-cooperative household framework. This modeling choice is motivated by two empirical regularities: the observed kink in time allocation at the equal-

[10] Observations implying hourly wages above \$100 are dropped due to top-coding truncation.

[11] The wage-share variable is trimmed to the interval $(0.25, 0.75)$ to avoid sparse extreme observations.

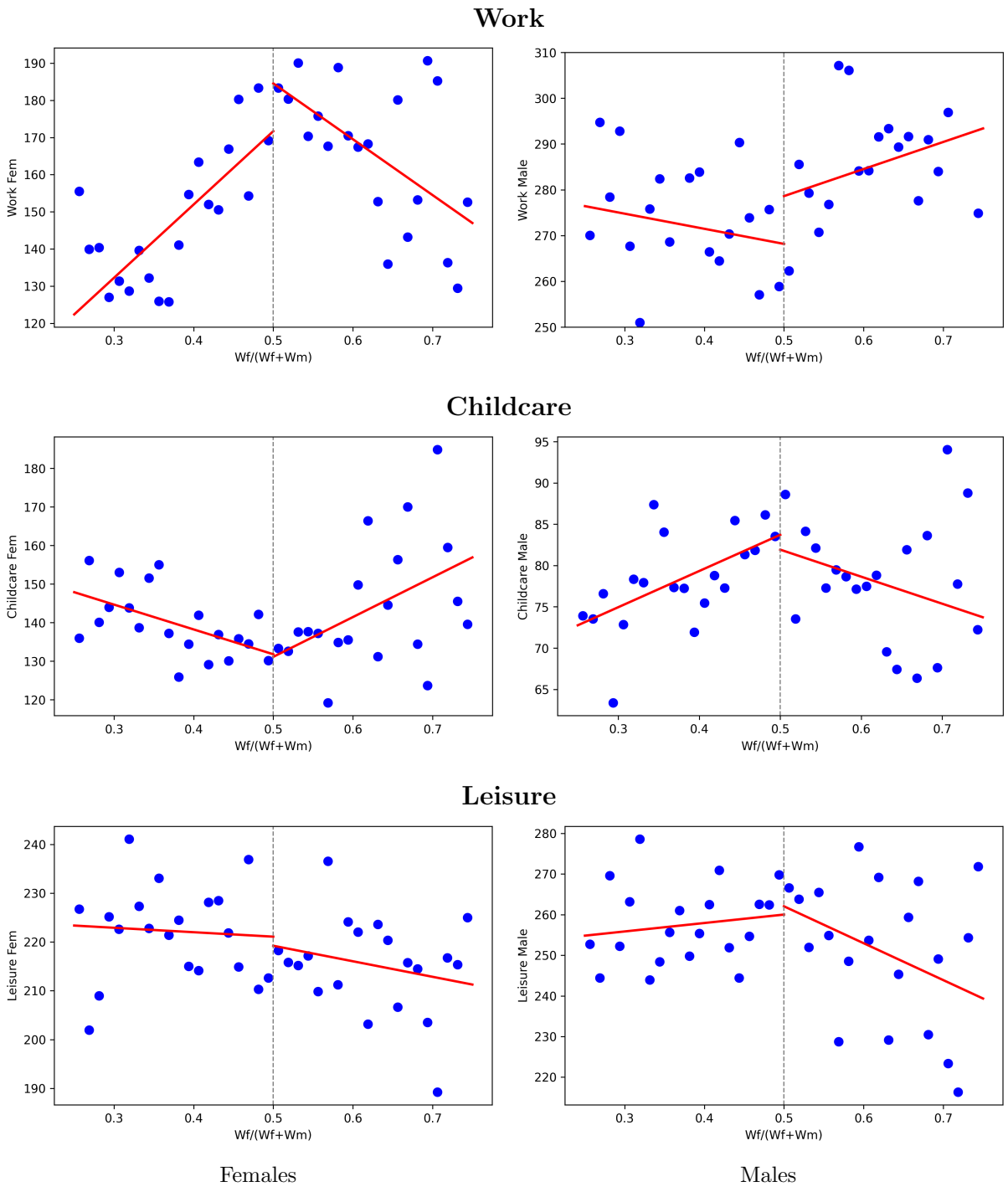

Figure 5: Relationship between a wife's wage share and average daily minutes devoted to work, childcare, and leisure. The figure plots local averages and linear fits allowed to kink at 0.5.

wage threshold and the prevalence of corner solutions in childcare (where one parent provides zero hours on the diary day). Standard fully cooperative collective models tend to smooth out these discontinuities unless ad-hoc frictions are introduced. A semi-cooperative setup, by contrast, treats market hours as contractible (jointly chosen) but models childcare as a privately provided public good chosen non-cooperatively. This structure naturally generates best-response functions with "flat" zero regions—reflecting strategic free-riding when the spouse's investment is sufficient—thereby reproducing the observed kinks and corners with minimal structural assumptions.

A household consists of two members, $i \in \{f, m\}$, each characterized by a market wage rate w_i, caring for n children, and endowed with one unit of time. Family members engage in a two-stage game. In the first stage, they jointly determine their optimal market labor supply; in the second stage, each individually chooses the time allocated to childcare.

Time budget. Each individual faces the time constraint:

$$h_i + l_i + (t_i + \tilde{t}_i)\, n \leq 1, \quad h_i > 0,\ l_i > 0,\ t_i \geq 0,\ \tilde{t}_i > 0, \tag{11}$$

where h_i denotes market work time, l_i leisure time, t_i parental quality time invested per child, $\tilde{t}_i$ the fixed (non-quality) childcare time cost per child, and n the number of children. Note that while market work and leisure are assumed strictly positive, quality time t_i allows for corner solutions ($t_i \geq 0$).

The quality of children is determined by a Cobb-Douglas production function:

$$q = (1 + t_f)^{\alpha}\, (1 + t_m)^{1-\alpha}, \tag{12}$$

with $\alpha \in [0, 1]$ governing the relative effectiveness of maternal versus paternal time inputs. Following Del Boca et al. (2013), consumption goods are assumed to have a negligible effect on child quality; thus, only time inputs enter the production function, a specification that facilitates the emergence of corner solutions in optimal childcare supply.

Utility and identity norm. Individual i's baseline utility is given by:

$$u_i \;=\; \log(c) \;+\; \mu_i \log(l_i) \;+\; \gamma_i \log(q\, n). \tag{13}$$

Following the social-norm tax frameworks of Greenwood et al. (2016)[12] and Doepke and Kindermann (2019)[13], consumable income is adjusted by a norm-dependent tax on the wife's earnings:

$$c \;=\; \phi(s)\, w_f h_f \;+\; w_m h_m, \qquad s \;=\; \frac{w_f}{w_f + w_m}. \tag{14}$$

In this model, the "identity backlash" emerges as the wife's share of potential household income approaches that of her husband. Accordingly, the social-norm tax is specified as a nonlinear, endogenous function of the wife's relative income share s:

$$\phi(s) \;=\; \exp\!\big[-\chi\, s^{\kappa}\big], \quad \chi > 0,\ \kappa > 1.$$

Unlike previous formulations, the tax rate here depends non-linearly on s. This ensures that social costs materialize primarily once the wife's wage share crosses a threshold determined by the curvature parameters χ and κ, while keeping consumption strictly positive.

Stages. Agents play a two-stage semi-cooperative game à la Cournot, solved by backward induction.

Stage 2 (Childcare): Taking market hours h_i as given from the first stage, each individual i maximizes their private utility with respect to t_i:

$$v_i(t_i, t_{-i} \mid h) = \log(c) \;+\; \mu_i \log\!\big(1 - h_i - (t_i + \tilde{t}_i)\, n\big) \;+\; \gamma_i \log\!\big((1+t_f)^{\alpha}(1+t_m)^{1-\alpha} n\big). \tag{15}$$

This stage results in four possible regimes: both, one, or neither spouse provides quality childcare time.

Stage 1 (Market Work): In the first stage, agents cooperatively choose market hours to maximize the household utility function, anticipating the Nash equilibrium outcomes of the second stage. The household objective is the weighted sum of individual utilities:

$$u_h \;=\; \theta\, u_f \;+\; (1-\theta)\, u_m,$$

where $\theta \in (0,1)$ denotes the bargaining power of the wife.

Under mild regularity conditions, this game admits a unique subgame perfect equilibrium. Since each spouse's time-allocation choice in Stage 2 solves a strictly concave maximization

[12] They specify household resources as $c = (1-\tau_t) w_f h_f + w_m h_m$, where τ_t is an exogenous, time-varying tax capturing gradually weakening anti-work norms against women.

[13] They model fertility bargaining by assigning the wife a constant cost share $\chi^f > 0$ of child-rearing expenditures. A larger χ^f, interpreted as a stricter gender norm, acts as a multiplicative wedge on her earnings.

problem over a compact, convex set:

$$\{t_i \geq 0 : \ h_i + l_i + (t_i + \tilde{t}_i)n \leq 1\},$$

Rosen's existence theorem ensures a unique Nash equilibrium in childcare for any given pair of market hours. In Stage 1, the induced household payoff is maximized. Since the utility function is continuous in (h_f, h_m) and diagonally strictly concave, Brouwer's fixed-point theorem ensures existence, while the diagonal strict concavity ensures the uniqueness of the profile $(h_f^*, h_m^*, t_f^*, t_m^*)$. Thus, the model admits exactly one equilibrium. Depending on the second-stage outcome, the solution falls into one of the twelve profiles reported in Appendix Section C.

Assumptions. A1 (Primitives). Preferences are defined as in (13) with parameters $\mu_i > 0$, $\gamma_i > 0$, $\alpha \in (0,1)$, wages $w_i > 0$, number of children $n \in \mathbb{N}$, and fixed time costs $\tilde{t}_i \geq 0$ such that the time budget is feasible $(1 - n\tilde{t}_i > 0)$ for $i \in \{f, m\}$.
A2 (Norm wedge). The function $\phi : [0,1] \to (0,1]$ is C^2, strictly decreasing, and log-convex in s (e.g., $\phi(s) = \exp[-\chi s^\kappa]$ with $\chi > 0, \kappa > 1$). When s is defined on *earnings* (endogenous), the mapping $(h_f, h_m) \mapsto \log(\phi(s) w_f h_f + w_m h_m)$ is strictly concave on the feasible set.[14]
A3 (Feasible sets). For any (h_f, h_m) such that $0 \leq h_i \leq 1 - n\tilde{t}_i$, each player's second-stage choice set for t_i is nonempty, convex, and compact. The joint feasible set for (h_f, h_m, t_f, t_m) is also nonempty, convex, and compact.

Proposition 1 (Existence and uniqueness)**.** *Under Assumptions A1–A3:*

(i) ***Stage 2 (Childcare).*** *For any pair of market hours (h_f, h_m), the second-stage game in (t_f, t_m) is a diagonally strictly concave game. Therefore, it admits a* unique *Nash equilibrium (t_f^*, t_m^*), and the equilibrium correspondence $(t_f^*, t_m^*)(h_f, h_m)$ is single-valued and continuous.*

(ii) ***Stage 1 (Market work).*** *Let $V(h_f, h_m) = \theta\, v_f\big(h_f, h_m, t^*\big) + (1-\theta)\, v_m\big(h_f, h_m, t^*\big)$ denote the household objective induced by the unique Stage 2 equilibrium. Under A2, V is strictly concave on the feasible set of (h_f, h_m); therefore, the Stage 1 problem has a* unique *maximizer (h_f^*, h_m^*).*

Consequently, the two-stage semi-cooperative problem has a unique *subgame-perfect equilibrium $(h_f^*, h_m^*, t_f^*, t_m^*)$.*

[14] A sufficient condition (proved in Appendix C.1) is $\chi \leq \bar{\chi}(\kappa, w_f, w_m, \underline{h}, \overline{h})$ given the bounds $0 < \underline{h} \leq h_i \leq \overline{h} < 1$ implied by the time constraint. If s is defined on *potential shares* (exogenous), ϕ is independent of (h_f, h_m) and strict concavity is immediate.

4.3 Estimation

The model is estimated to replicate observed patterns in women's market work, childcare time, and their share of household wages. Wages and the number of children are drawn from log-normal distributions parameterized using summary statistics from the ATUS sample (Table 6).[15]

Table 6: Summary statistics for simulation inputs

Variable	Mean	Std. Dev.
Female wages (w_f)	16.309	9.366
Male wages (w_m)	18.904	10.084
Number of children (n)	2.105	0.978

The bargaining power parameter, θ_i, is assumed to follow a logistic-normal distribution:

$$\theta_i \;=\; \frac{1}{1+\exp(-z_i)}, \qquad z_i \;\sim\; \mathcal{N}\big(\bar{\theta},\, \sigma^2\big),$$

which ensures $\theta_i \in (0,1)$. Here, $\bar{\theta}$ and σ^2 denote the mean and variance of the underlying normal distribution, respectively.

The preference weight for consumption is normalized to unity. With log utility, only the ratios between the preference weights on consumption, leisure, and child quality are identified by time-use moments; scaling all utility weights by a constant leaves choices unchanged. Since consumption quantities are unobserved, fixing the consumption weight anchors the utility scale and avoids weak identification. The child-quality productivity parameter, α, is fixed at 0.5, following Del Boca et al. (2013) and Gobbi (2018). The remaining parameters,

$$\Theta = (\gamma_f,\, \gamma_m,\, \mu_f,\, \mu_m,\, \tilde{t}_f,\, \tilde{t}_m,\, \bar{\theta},\, \sigma,\, \chi,\, \kappa),$$

are estimated via the Method of Simulated Moments (MSM). Formally, the estimator minimizes the weighted distance between data and model moments:

$$\hat{\Theta} = \arg\min_{\Theta} \left(\frac{m-\hat{m}(\Theta)}{m}\right)' W \left(\frac{m-\hat{m}(\Theta)}{m}\right), \tag{16}$$

where m stacks the mean shares of time allocated to market work and childcare across five bins of the wife's relative wage share, $s = \frac{w_f}{w_f+w_m} \in (0.25, 0.75)$, yielding 20 moments in total.

I employ the identity weighting matrix, $W = I$, for three primary reasons: (i) the targeted

[15] Nominal wages are deflated to constant-2000 dollars.

moments are standardized as percentage deviations, making equal weighting effectively close to efficient; (ii) ATUS diary measures are zero-inflated and heteroskedastic, with sparsity in some bins making the empirical covariance matrix noisy and potentially ill-conditioned; and (iii) the identity matrix yields a smoother objective function, improving the stability of the optimization routine. The minimization is performed in two stages: a Differential Evolution search provides a global candidate minimum, which then seeds a local quadratic-approximation routine.

Table 7 presents the parameter estimates obtained by simulating 50,000 households, both for the full model ($\phi \neq 1$) and the restricted model without the social norm ($\phi = 1$). In the baseline specification, the logistic-normal parameters ($\bar{\theta} = -0.45$) imply an average female Pareto weight of approximately 0.43. This estimate is consistent with the broader collective household literature, which typically estimates female bargaining weights below 0.5 (Knowles, 2013; Friedberg and Webb, 2006).

In contrast, estimating the model without the identity norm ($\phi = 1$) yields a positive mean for the underlying distribution ($\bar{\theta} = 0.35$), implying an average female Pareto weight of approximately 0.56. This counter-intuitive result suggests that, in the absence of the identity mechanism, the model must attribute an unrealistically high bargaining power to women to rationalize their observed labor supply choices. By explicitly modeling the identity cost, the benchmark model recovers bargaining parameters that align more closely with external empirical evidence, providing further support for the identity mechanism as a driver of intra-household allocation.

Table 7: Structural parameter estimates

Parameter	Description	Estimates	
		Benchmark ($\phi \neq 1$)	No Norm ($\phi = 1$)
γ_f, γ_m	Preferences for child quality	3.67, 4.48	1.49, 4.02
$\tilde{t}_f, \tilde{t}_m$	Fixed childcare time cost	0.09, 0.05	0.08, 0.06
μ_f, μ_m	Preferences for leisure	1.19, 1.11	1.15, 1.37
$\bar{\theta}, \sigma$	Bargaining power (z_i distrib.)	-0.45, 1.98	0.35, 1.75
κ, χ	Identity norm parameters	4.19, 7.27	–

4.4 Numerical results

Using the estimated parameters, this section first compares the simulated moments with those targeted in the estimation. It then presents counterfactual analyses demonstrating how households respond to wage shocks at different points in the income distribution.

4.4.1 Comparison with data

Table 8 compares the empirical averages for time spent working, childcare, and employment rates with those generated by the model using the benchmark parameters (Table 7). The model closely replicates the observed time-allocation patterns. On average, men allocate approximately half of their time budget to market work and 12% to childcare, matching the data almost exactly. For women, the model captures the division of labor well, predicting a market work share of 26% (data: 24%) and a childcare share of 22% (data: 23%).

Crucially, the comparison with the "No Norm" specification ($\phi = 1$) highlights the necessity of the identity mechanism. Without the norm, the model struggles to fit the gendered division of labor simultaneously with employment rates. It underestimates male market work (0.44 vs. 0.47) while overestimating female market work (0.30 vs. 0.24). Furthermore, the benchmark model successfully generates a high male employment rate (99.9%) and a lower female employment rate (57%), qualitatively matching the empirical gap (97% vs. 68%), despite employment rates being untargeted external moments.

Table 8: Comparison of model and data averages

Sex	Moment	Model mean ($\phi \neq 1$)	Model mean ($\phi = 1$)	Data mean
Internal moments (Targeted)				
Male	Work	0.4989	0.4360	0.4709
	Childcare	0.1207	0.1303	0.1280
Female	Work	0.2608	0.3006	0.2443
	Childcare	0.2210	0.1755	0.2342
External moments (Untargeted)				
Male	Employment	0.9999	0.8543	0.9715
Female	Employment	0.5663	0.7163	0.6775

Figure 6 plots the simulated time-use profiles for market work and childcare across five bins of the wife's wage share, juxtaposed with the ATUS data. The model successfully reproduces the key non-monotonicities documented in Section 4.1. Specifically, it captures the **inverse-V shape** in women's labor supply: market hours rise as the wife's relative wage increases toward parity, but visibly decline once she becomes the primary earner. Similarly, the model replicates the **V-shaped** trough in female childcare and the corresponding spikes in male market work beyond the equal-earnings threshold. This structural fit confirms that the estimated identity cost is sufficient to generate the "kinked" behavioral responses observed in the data.

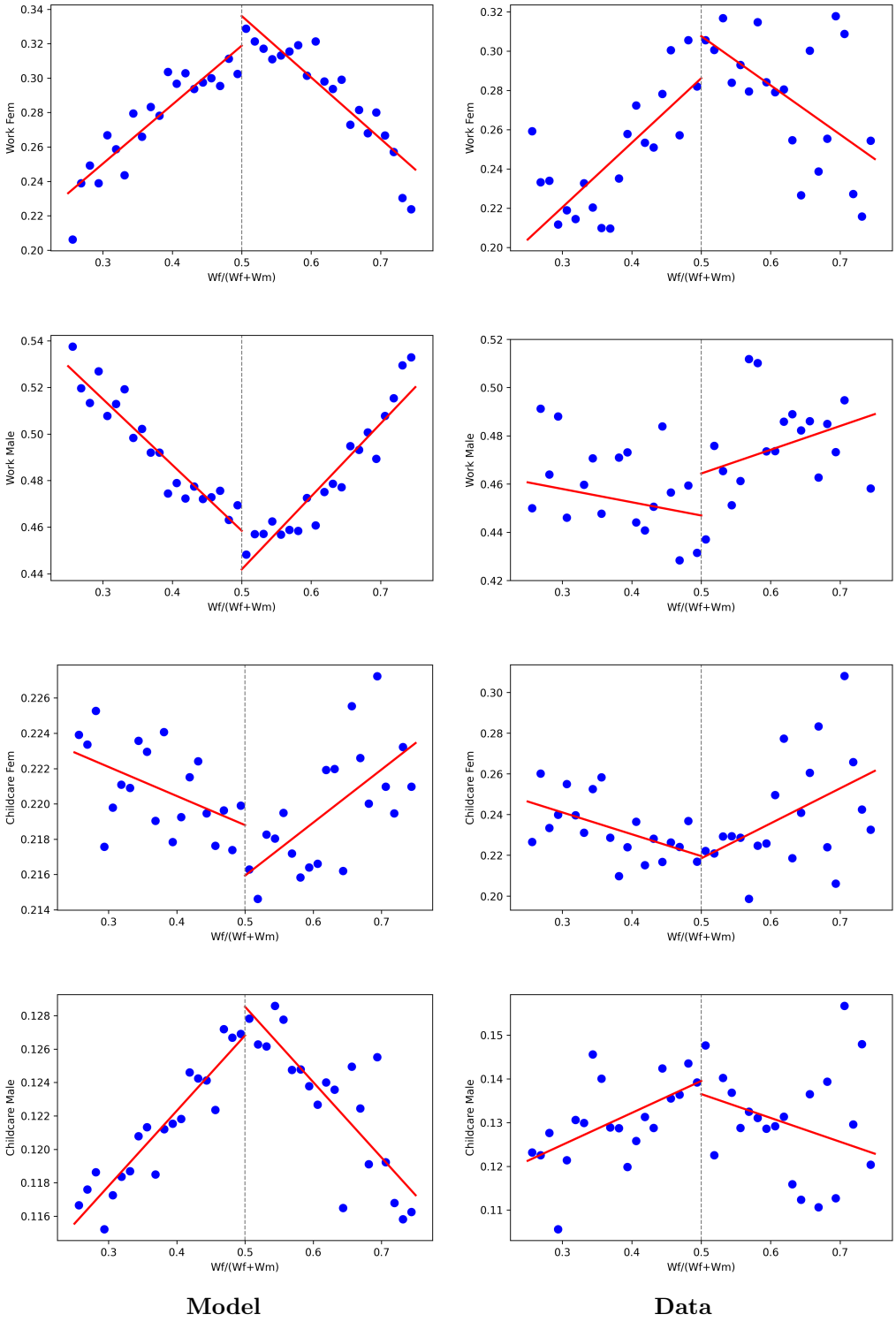

Figure 6: Simulated vs. observed time shares for work and childcare across the distribution of the wife's wage share.

4.4.2 Counterfactuals

Empirical studies of the U.S. robot wave show that the observed narrowing of the gender wage gap is driven primarily by declining earnings—or outright job loss—among men in the bottom-to-middle terciles, whereas compression on the female side arises from modest gains concentrated in the upper terciles of the female distribution (see, e.g., Acemoglu and Restrepo, 2020; Cortes et al., 2024).

To replicate this pattern quantitatively, I consider wage shocks targeting the bottom tercile of the male wage distribution. A key challenge in calibrating these shocks is that empirical estimates typically measure effects on *observed* wages among employed workers. However, in the structural model, agents respond to changes in their *potential* market wage, which governs decisions on both the intensive (hours worked) and extensive (participation) margins.

Since exposure to robots generates significant displacement (non-employment), relying solely on observed wage declines would understate the true shock to men's labor market opportunities due to positive selection bias—i.e., the lowest-productivity workers exit the sample, mechanically propping up the average observed wage. Therefore, I calibrate the model shocks to match the *total earnings effect*, combining the decline in hourly wages with the decline in the probability of employment. Formally, the percentage change in potential earnings is approximated as:

$$\Delta\%w_{pot} \approx \underbrace{(\text{Exposure} \times \beta_{wage})}_{\text{Intensive Margin}} + \underbrace{\left(\frac{\text{Exposure} \times \beta_{emp}}{\text{Base Employment Rate}}\right)}_{\text{Extensive Margin}} \tag{17}$$

where β_{wage} is the semi-elasticity of wages and β_{emp} is the marginal effect on the employment-to-population ratio.

Automation Shock. For the robot counterfactual, I simulate a "high-exposure" scenario of **3 additional robots per 1,000 workers**. This magnitude is representative of the "Rust Belt" experience (e.g., commuting zones in Michigan and Ohio), which drove the aggregate displacement results in Acemoglu and Restrepo (2020).

Using estimates for men with less than a college degree ($\beta_{wage} \approx -0.008$; $\beta_{emp} \approx -0.005$) and the 1990 baseline non-college male employment rate of 0.80,[16] the intensive margin shock is -2.4% (3×-0.008). The extensive margin shock contributes an additional -1.9% decline

[16] According to BLS historical data for 1990, the employment-to-population ratio for prime-age men with a high school diploma fluctuated between 0.78 and 0.82. Since the Acemoglu and Restrepo (2020) sample begins in 1990, 0.80 serves as the appropriate demographic baseline.

$(3 \times -0.005/0.80)$. The sum yields a total potential earnings decline of roughly -4.3%. Accordingly, I calibrate the robot counterfactual as a **4% decline** in potential wages for men in the first tercile.

Female Wage Complementarity. In addition to the negative shocks to male earnings, it is reasonable to expect an accompanying positive variation in the potential wages of women in the upper tail of the distribution. Unlike the direct displacement experienced by low-skill men, the effect on high-skill women operates through *occupational upgrading* and *sectoral reallocation*.

Cortes et al. (2024) find that in automation-exposed labor markets, women are significantly more likely than men to transition out of routine tasks and into cognitive, high-wage occupations. While the counterfactuals presented below conservatively isolate the decline in male opportunity costs, these studies suggest a complementarity premium for women—potentially in the range of 2%—which would act as a mirroring force, accelerating the convergence of spousal relative earnings and amplifying the identity mechanism.

Simulation Results. Figure 7 plots the divergence in time use—specifically the gender gaps in market work $(h_m - h_f)$ and childcare $(t_f - t_m)$—across the range of wage shocks.

For the **4% automation shock**, the distortionary effect of the norm is already visible. In the identity-neutral benchmark, the gender gap in market work remains relatively stable, as the substitution effect is offset by income effects. However, under the identity norm, the gender work gap widens from a baseline of 0.238 to 0.242—an increase of approximately 1.7%. This divergence drives the "identity distortion" up by roughly **2%**.

The right panel displays the corresponding dynamics for childcare $(t_f - t_m)$. While allocations here are more rigid due to fixed time costs, the inefficiency persists: the norm prevents the narrowing of the childcare gap that would naturally occur as men's relative opportunity cost of time falls.

Finally, it is reasonable to expect that the total impact of these structural shocks exceeds the magnitudes illustrated in Figure 7. The figure isolates the effect of the male wage decline; however, as discussed, automation often induces a simultaneous positive shock to female wages via occupational upgrading. Since the identity norm responds to the *ratio* of spousal earnings, a simultaneous increase in female wages acts as a mirroring force, accelerating the convergence to the breadwinner threshold. Consequently, the combined effect of collapsing male opportunity costs and rising female potential earnings would likely generate distortions in time allocation significantly larger than the conservative estimates reported here.

The calibrated semi-cooperative model formalizes the causal intuition for the results

presented in Section 3. A negative shock to men's wages raises the wife's wage share and, through the identity cost embedded in the consumption aggregator, creates an endogenous threshold $s^\star$ around equal earnings. Below $s^\star$, standard labor-supply forces dominate and women's market hours rise with their relative wage; above $s^\star$, the identity cost reduces the marginal payoff to additional female market hours, flipping the slope and shifting time into childcare and leisure. Because the size of the wage-share shift is greatest near or above parity, aggregate effects scale nonlinearly with the cross-household distribution of relative wages: counterfactuals show that the share of couples for which the norm binds increases when shocks compress the gender wage gap, systematically amplifying gaps in time use.

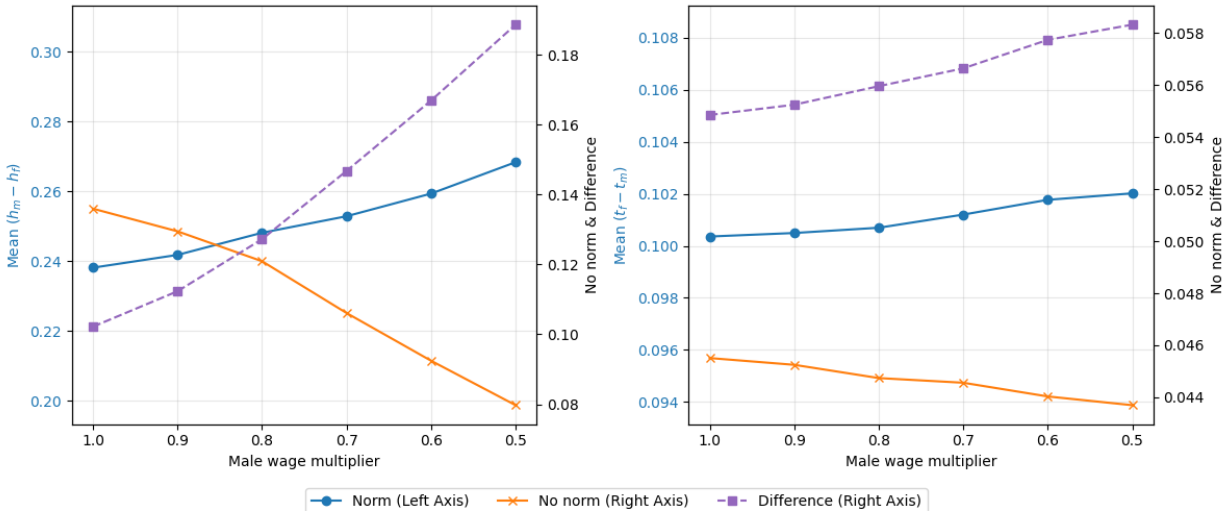

Figure 7: Simulated divergence in time use gaps in response to negative shocks to first-tercile male wages. The left panel shows the gender gap in market work ($h_m - h_f$); the right panel shows the gender gap in childcare ($t_f - t_m$). The x-axis represents the multiplier applied to male wages (e.g., 0.96 corresponds to a 4% shock).

5 Conclusion

This paper examines how industrial automation reshapes the allocation of time within households. By linking ATUS time diaries to commuting-zone exposure to robots and addressing endogeneity with external industry shifters, I document systematic within-couple reallocations. Greater exposure to robots leads women to shift time out of market work and into childcare and leisure, while men simultaneously increase market work and reduce leisure. Quantitatively, one additional robot per 1,000 workers reallocates roughly one hour per week at the household level across work, childcare, and leisure.

These empirical patterns are rationalized by a structural household model featuring an identity norm that penalizes couples when the wife out-earns the husband. The model

reproduces the observed non-monotonicity in time use: as the wife's potential wage share rises toward parity, her market hours increase; however, once the breadwinner threshold is crossed, the identity cost triggers a withdrawal from the labor market and a sharp increase in childcare time. Counterfactual simulations indicate that this norm roughly doubles the gender gap in market hours relative to an identity-neutral benchmark. Crucially, because automation shocks disproportionately depress men's wages in the lower-middle of the distribution, they push a significant mass of couples into the region where this norm binds, amplifying gender gaps in time use even as the raw wage gap narrows.

The findings highlight that cultural norms can act as a substantial friction, preventing the efficient allocation of time following economic shocks. This suggests several avenues for policy intervention.

First, policies that subsidize substitutes for home production can weaken the identity mechanism. Since the norm manifests primarily through the substitution of female market work for childcare, policies that lower the cost of childcare and early education are particularly relevant. If high-quality external care is affordable and accessible, the relative price of specializing in home production rises, potentially offsetting the "identity tax" that discourages women from working when their husbands' earnings fall.

Second, the results provide a novel argument for targeted wage insurance. Standard adjustment assistance often focuses on retraining displaced workers. However, this paper shows that a drop in the husband's wage can trigger a secondary withdrawal of the wife from the labor force. Wage insurance schemes that shore up the earnings of displaced male workers could, counter-intuitively, prevent the decline of female labor supply by keeping households away from the identity discontinuity where the breadwinner norm binds.

Third, place-based policies must account for the gendered nature of local demand shocks. Regional development policies often aim to restore manufacturing jobs. However, given the structural shift toward services—where women often hold a comparative advantage—development strategies should also facilitate the transition of men into service-sector roles. Reducing the strong gender segregation of occupations would align labor demand with household supply and, over the long term, potentially soften the rigidity of identity norms.

In sum, automation does not only reallocate tasks across firms; it reallocates time within households. When relative wages move couples toward earnings parity, social norms can paradoxically reverse progress in gender equality. Recognizing and quantifying this interaction is essential for designing policies that ensure the benefits of technological change are distributed efficiently within the family.

References

Acemoglu, D. and Restrepo, P. (2020). Robots and jobs: Evidence from us labor markets. *Journal of Political Economy*, 128(6):2188–2244.

Adão, R., Kolesár, M., and Morales, E. (2019). Shift-share designs: Theory and inference*. *The Quarterly Journal of Economics*, 134(4):1949–2010.

Anelli, M., Giuntella, O., and Stella, L. (2021). Robots, marriageable men, family, and fertility. *Journal of Human Resources*, page 1020.

Autor, D., Dorn, D., and Hanson, G. (2019). When work disappears: Manufacturing decline and the falling marriage market value of young men. *American Economic Review: Insights*, 1(2):161–78.

Autor, D. H. and Dorn, D. (2013). The growth of low-skill service jobs and the polarization of the us labor market. *American Economic Review*, 103(5):1553–97.

Autor, D. H., Dorn, D., and Hanson, G. H. (2013). The china syndrome: Local labor market effects of import competition in the united states. *American Economic Review*, 103(6):2121–68.

Becker, G. S. (1965). A theory of the allocation of time. *The Economic Journal*, 75(299):493–517.

Bertrand, M., Kamenica, E., and Pan, J. (2015). Gender identity and relative income within households. *The Quarterly Journal of Economics*, 130(2):571–614.

Besedeš, T., Lee, S. H., and Yang, T. (2021). Trade liberalization and gender gaps in local labor market outcomes: Dimensions of adjustment in the united states. *Journal of Economic Behavior & Organization*, 183:574–588.

Bick, A. and Fuchs-Schündeln, N. (2018). Taxation and labor supply of married couples across countries: A macroeconomic analysis. *American Economic Review*, 108(6):1543–76.

Blundell, R., Pistaferri, L., and Saporta-Eksten, I. (2018). Children, Time Allocation, and Consumption Insurance. *Journal of Political Economy*, 126(S1):73–115.

Chetty, R., Guryan, J., Kroft, K., and Looney, A. (2011). Are micro and macro labor supply elasticities consistent? a review of evidence on the intensive margin. *American Economic Review*, 101(3):471–75.

Chiappori, P.-A. (1992). Collective labor supply and welfare. *Journal of Political Economy*, 100(3):437–467.

Cortes, P., Feng, Y., Guida-Johnson, N., and Pan, J. (2024). Automation and gender: Implications for occupational segregation and the gender skill gap. NBER Working Paper 32030, National Bureau of Economic Research.

Costanzo, C. (2025). Robots, jobs, and optimal fertility timing. *Journal of Population Economics*, 38(2):1–33.

de Vries, G. J., Gentile, E., Miroudot, S., and Wacker, K. M. (2020). The rise of robots and the fall of routine jobs. *Labour Economics*, 66:101885.

Del Boca, D., Flinn, C., and Wiswall, M. (2013). Household Choices and Child Development. *The Review of Economic Studies*, 81(1):137–185.

Doepke, M. and Kindermann, F. (2019). Bargaining over babies: Theory, evidence, and policy implications. *American Economic Review*, 109(9):3264–3306.

Flood, S., King, M., Rodgers, R., Ruggles, S., Warren, J. R., Backman, D., Chen, A., Cooper, G., Richards, S., Schouweiler, M., and Westberry, M. (2024). IPUMS CPS: Version 12.0 [dataset]. Minneapolis, MN: IPUMS.

Friedberg, L. and Webb, A. (2006). Determinants of intra-household bargaining power. *American Economic Review*, 100(2):224–224.

Ge, S. and Zhou, Y. (2020). Robots, computers, and the gender wage gap. *Journal of Economic Behavior & Organization*, 178:194–222.

Giuntella, O., Lu, Y., and Wang, T. (2024). How do workers adjust to robots? evidence from china. *The Economic Journal*, 135(666):637–652.

Glass, J. and Nath, L. E. (2006). Religious conservatism and women's market behavior following marriage and childbirth. *Journal of Marriage and Family*, 68(3):611–629.

Gobbi, P. E. (2018). Childcare and commitment within households. *Journal of Economic Theory*, 176:503–551.

Goldsmith-Pinkham, P., Sorkin, I., and Swift, H. (2020). Bartik instruments: What, when, why, and how. *American Economic Review*, 110(8):2586–2624.

Greenwood, J., Guner, N., Kocharkov, G., and Santos, C. (2016). Technology and the changing family: A unified model of marriage, divorce, educational attainment, and female labor-force participation. *The Review of Economic Studies*, 83(1):157–199.

Guiso, L., Sapienza, P., and Zingales, L. (2003). People's opium? religion and economic attitudes. *Journal of Monetary Economics*, 50(1):225–282.

Halla, M., Schmieder, J., and Weber, A. (2020). Job displacement, family dynamics, and spousal labor supply. *American Economic Journal: Applied Economics*, 12(4):253–87.

Hamermesh, D. S., Frazis, H., and Stewart, J. (2005). Data watch: The american time use survey. *Journal of Economic Perspectives*, 19(1):221–232.

Heggeness, M. and Murray-Close, M. (2019). Manning up and womaning down: How husbands and wives report earnings when she earns more. Opportunity and Inclusive Growth Institute Working Papers 28, Federal Reserve Bank of Minneapolis.

ISSP Research Group (2016). International social survey programme: Family and changing gender roles iv - issp 2012. GESIS Datenarchiv, Köln. Available online at https://doi.org/10.4232/1.12661.

Kleibergen, F. and Paap, R. (2006). Generalized reduced rank tests using the singular value decomposition. *Journal of Econometrics*, 133(1):97–126.

Knowles, J. (2013). Why are married men working so much? an aggregate analysis of intra-household bargaining and labor supply. *The Review of Economic Studies*, 80(3):1055–1085.

Matysiak, A., Bellani, D., and Bogusz, H. (2023). Industrial robots and regional fertility in European countries. *European Journal of Population*, 39(1):11.

Rosenberg, S. (2021). Revisiting the Breadwinner Norm: The effect of potential relative earnings on married women's labor supply. Manuscript, ECARES, Université Libre de Bruxelles.

Stephens Jr., M. (2001). The long-run consumption effects of earnings shocks. *Review of Economics and Statistics*, 83(1):28–36. Note: Often cited as 2002 in working paper versions, but published 2001 in REStat or 2002 in JPE depending on the specific focus. The JPE 2002 paper 'Worker Displacement and the Added Worker Effect' is likely the specific one you want for labor supply.

Stephens Jr., M. (2002). Worker displacement and the added worker effect. *Journal of Political Economy*, 110(3):504–541.

Stewart, J. (2013). Tobit or not tobit? *Journal of Economic and Social Measurement*, 38(3):263–290.

van Ark, B. and Jäger, K. (2017). Recent trends in europe's output and productivity growth performance at the sector level, 2002-2015. *International Productivity Monitor*, 33:8–23.

Webb, M. (2019). The Impact of Artificial Intelligence on the Labor Market.

Zinovyeva, N. and Tverdostup, M. (2021). Gender identity, coworking spouses, and relative income within households. *American Economic Journal: Applied Economics*, 13(4):258–84.

Acknowledgements I am grateful to Paula Gobbi, Bram De Rock, Fabio Blasutto, David Hémous, Luke Heath Milsom, as well as seminar participants at ULB–ECARES, KU-Leuven and UZH for their helpful comments.

Funding This project has been funded by the Belgian National Fund for Scientific Research (FNRS).

Data availability The following data sources have been used for the analysis in this article:

- **American Time Use Survey (ATUS)** – U.S. Bureau of Labor Statistics, 2003–2023.
- **Current Population Survey (CPS)** – ASEC and basic monthly files, via IPUMS-CPS (Flood et al. 2024 release); 1990–2023.
- **ISSP "Family and Changing Gender Roles IV"** – 2012 U.S. subsample.
- Patent-based automation-risk scores – Webb (2020, *American Economic Review: Insights* 2(3): 300-17).
- O*NET manual-task intensity scores – Autor & Dorn (2013, *AER* 103(5): 1553-97).
- 1990 commuting-zone × industry employment shares – Acemoglu & Restrepo (2020, *JPE* 128(6): 2188-2244).
- 1970 commuting-zone × industry employment shares – Decennial IPUMS data.
- Industrial-robot stocks (country × industry, 1993-2019) – International Federation of Robotics, *World Robotics* database.
- 1990 industry employment for EU-5 (used in the robot instrument) – EU KLEMS Growth & Productivity Accounts, 2017 edition.
- U.S. import-exposure, domestic absorption and baseline instrument files – Autor, Dorn & Hanson (2013, "The China Syndrome," *AER* 103(6): 2121-68).
- Chinese exports to eight alternative OECD markets – UN Comtrade extraction following Autor–Dorn–Hanson.
- Commuting-zone boundaries and county cross-walks – Autor, Dorn & Hanson replication materials (2013).

Conflict of interest The author declares that he has no conflict of interest.

Appendix

A Supplementary tables

Table A1: Descriptive statistics: ATUS general population

	Females			Males		
Variable	Obs	Mean	Std. Dev.	Obs	Mean	Std. Dev.
Leisure (min/day)	122,710	310.07	208.33	96,658	356.87	235.57
Childcare (min/day)	122,710	43.10	101.62	96,658	22.34	69.34
Market work (min/day)	122,710	126.61	217.06	96,658	191.39	261.12
Age	122,710	48.37	18.15	96,658	46.77	17.44
Hourly wage (USD)	35,769	15.08	9.23	29,080	17.52	10.25
Weekly earnings (USD)	61,698	709.03	513.95	54,518	951.10	596.42
Usual work hours per week	113,670	21.20	20.66	88,373	30.94	22.49
Less than secondary (%)	122,710	14.37	35.08	96,658	15.69	36.37
Secondary (%)	122,710	25.91	43.81	96,658	25.52	43.60
Some college (%)	122,710	27.95	44.87	96,658	25.39	43.52
Tertiary (%)	122,710	31.77	46.56	96,658	33.40	47.17

Notes: "General population" includes all ATUS respondents by sex. Variable definitions are as in Table 1.

Table A2: Effect of robots on time spent working, childcaring, and leisuring per day (2SLS). Sample: respondents with no spouse or unmarried partner.

	Males		Females	
	Work	Leisure	Work	Leisure
Robots	-1.030	5.324	7.234	-7.132*
	(6.457)	(5.137)	(4.652)	(4.314)
Observations	8,519	8,519	11,741	11,741
R-squared	0.318	0.246	0.312	0.187
Respondent employed	✓	✓	✓	✓

Notes: Controls include commuting zone and state-by-year FE, respondent's age/education, day, month, holiday. Standard errors clustered at the commuting-zone–year level. *** $p < 0.01$, ** $p < 0.05$, * $p < 0.1$.

Table A3: Effect of China shock on time spent working, childcaring, and leisuring per day (2SLS).

	Males			Females		
	(1)	(2)	(3)	(4)	(5)	(6)
Daily minutes work						
Trade	-6,464***	-5,944**	-5,106***	1,907	-2,062	-2,940**
	(1,809)	(2,391)	(1,550)	(1,192)	(1,380)	(1,433)
Observations	3,507	5,726	3,305	6,324	4,300	3,899
R-squared	0.431	0.431	0.512	0.272	0.402	0.460
Daily minutes childcare						
Trade	1,127	2,054	605.2	138.9	967.3	2,067**
	(873.1)	(1,477)	(825.9)	(656.8)	(795.3)	(853.1)
Observations	3,507	5,726	3,305	6,324	4,300	3,899
R-squared	0.225	0.171	0.316	0.227	0.226	0.283
Daily minutes leisure						
Trade	-389.9	469.2	-168.8	-1,453*	-784.9	-362.8
	(1,145)	(1,200)	(1,235)	(869.9)	(977.6)	(1,112)
Observations	3,507	5,726	3,305	6,324	4,300	3,899
R-squared	0.312	0.270	0.378	0.208	0.289	0.338
Spouse employed	✓		✓	✓		✓
Respondent employed		✓	✓		✓	✓

Notes: Sample: married or cohabiting couples with at least one spouse working and children aged 10 or less. Controls include state-by-year FE, demographic/household controls, day/month/holiday FE. Standard errors clustered at the commuting-zone–year level. *** $p < 0.01$, ** $p < 0.05$, * $p < 0.1$.

Table A4: Effect of decomposed China shock on time spent working, childcaring, and leisuring per day (2SLS).

	Males			Females		
	(1)	(2)	(3)	(4)	(5)	(6)
Daily minutes work						
Trade_{Male}	12,104	3,581	8,834	3,027	-1,340	-4,278
	(8,036)	(5,805)	(7,418)	(5,362)	(7,632)	(8,164)
Trade_{Fem}	-34,282***	-20,546**	-27,758**	-476.7	-3,874	-1,475
	(12,443)	(9,692)	(12,004)	(8,515)	(12,102)	(13,134)
Daily minutes childcare						
Trade_{Male}	6,228	4,300	7,127*	-2,684	-1,603	-2,293
	(3,924)	(2,843)	(3,655)	(3,261)	(3,590)	(4,392)
Trade_{Fem}	-6,492	-1,309	-9,280	4,910	5,079	8,939
	(5,678)	(4,613)	(5,695)	(5,229)	(5,832)	(7,029)
Daily minutes leisure						
Trade_{Male}	-17,611***	-5,883	-14,711***	-809.3	2,043	426.1
	(5,484)	(3,835)	(5,416)	(4,216)	(4,775)	(5,188)
Trade_{Fem}	25,302***	10,115	21,618**	-2,451	-5,012	-1,888
	(8,742)	(6,177)	(8,664)	(6,495)	(7,639)	(8,234)
Spouse employed	✓		✓	✓		✓
Respondent employed		✓	✓		✓	✓

Notes: Sample includes married or cohabiting couples with at least one spouse working and children aged 10 or less. All specifications use 2SLS. Standard errors clustered at the commuting-zone–year level. *** $p < 0.01$, ** $p < 0.05$, * $p < 0.1$.

Table A5: Joint effects of robots and import competition on time spent working, childcaring, and leisuring per day (2SLS).

	Males			Females		
	(1)	(2)	(3)	(4)	(5)	(6)
Daily minutes work						
Robots	30.02***	18.57**	36.37***	-15.69*	-10.44	-16.63
	(8.493)	(8.177)	(8.249)	(8.660)	(12.94)	(14.47)
Trade	-7,383***	-7,244*	-6,401***	3,887*	-16.90	-920.8
	(2,661)	(3,742)	(2,147)	(2,169)	(2,729)	(2,862)
Observations	6,795	6,582	3,905	7,668	4,974	4,546
R-squared	0.426	0.455	0.529	0.297	0.430	0.476
Daily minutes childcare						
Robots	-0.547	1.337	-0.569	-2.966	2.308	1.579
	(3.474)	(3.902)	(3.376)	(5.544)	(6.428)	(7.178)
Trade	-1,089	-295.3	-1,556	-981.2	-622.6	123.0
	(1,321)	(1,829)	(1,254)	(1,150)	(1,487)	(1,545)
Observations	6,795	6,582	3,905	7,668	4,974	4,546
R-squared	0.170	0.179	0.323	0.230	0.232	0.290
Daily minutes leisure						
Robots	-7.832	-2.453	-12.69**	8.970	12.90*	17.83**
	(7.182)	(5.219)	(5.824)	(6.480)	(7.149)	(7.701)
Trade	-110.7	558.8	7.496	-1,701	974.0	857.0
	(1,926)	(1,797)	(1,624)	(1,555)	(1,776)	(1,829)
Spouse employed	✓		✓	✓		✓
Respondent employed		✓	✓		✓	✓

Notes: Sample includes married or cohabiting couples with at least one spouse working and children aged 10 or less. Control variables in all specifications include state-by-year fixed effects, demographic/household controls, day/month/holiday FE. Standard errors clustered at the commuting-zone–year level. *** $p < 0.01$, ** $p < 0.05$, * $p < 0.1$.

Table A6: Effect of Robot exposure on wages and wage gap (3, 5, and 7-year differences, 2SLS).

	3-Year Differences			**5-Year Differences**			**7-Year Differences**		
	(1) Male Wages	(2) Female Wages	(3) Wage Gap	(4) Male Wages	(5) Female Wages	(6) Wage Gap	(7) Male Wages	(8) Female Wages	(9) Wage Gap
Robots	-0.061***	-0.009	-0.050***	-0.025**	0.005	-0.027	-0.014**	0.004	-0.017*
	(0.011)	(0.010)	(0.013)	(0.010)	(0.012)	(0.018)	(0.006)	(0.008)	(0.009)
Observations	1,223	1,257	1,141	1,003	1,020	927	806	825	754
R^2	0.040	0.012	0.027	0.032	0.015	0.014	0.054	0.011	0.027

Notes: Sample: Working age individuals (25–54) in the ATUS. The dependent variable is the long difference (3, 5, or 7 years) of the log hourly wage for men, women, or the gender gap. All specifications include 1990 baseline controls and year fixed effects. Robust standard errors clustered at the commuting-zone level. *** $p < 0.01$, ** $p < 0.05$, * $p < 0.1$.

Table A7: Robustness to Sample Selection: Effect of robots on market work, childcare, and leisure using Inverse Probability Weighting (2SLS).

	Males			Females		
	(1)	(2)	(3)	(4)	(5)	(6)
Daily minutes work						
Robots	12.45**	4.831	12.90**	-14.73***	-18.38***	-17.04***
	(5.659)	(4.492)	(6.331)	(5.196)	(5.469)	(6.213)
Daily minutes childcare						
Robots	-0.589	2.086	0.377	5.898**	9.188***	8.682***
	(2.141)	(1.980)	(2.020)	(2.793)	(3.178)	(3.339)
Daily minutes leisure						
Robots	-3.784	-1.575	-8.405**	8.525**	13.55***	12.40***
	(4.512)	(3.474)	(3.509)	(3.481)	(3.451)	(4.149)
Spouse employed	✓		✓	✓		✓
Respondent employed		✓	✓		✓	✓

Notes: Controls include commuting zone and state-by-year FE, household controls, day/month/holiday. Sample: Individuals living with a spouse and children aged 10 or less. Standard errors clustered at the commuting-zone–year level. *** $p < 0.01$, ** $p < 0.05$, * $p < 0.1$.

Table A8: Effect of robot shock on hours worked per week (2SLS).

	Males			Females		
Weekly hours worked	(1)	(2)	(3)	(4)	(5)	(6)
Robots	-0.168	-0.0430	-0.159	-1.010**	-1.345***	-1.026**
	(0.316)	(0.203)	(0.286)	(0.464)	(0.390)	(0.421)
Spouse employed	✓		✓	✓		✓
Respondent employed		✓	✓		✓	✓

Notes: Controls include commuting zone and state-by-year FE, household controls, day/month/holiday. Sample: Individuals living with a spouse and children aged 10 or less. Standard errors clustered at the commuting-zone–year level. *** $p < 0.01$, ** $p < 0.05$, * $p < 0.1$.

Table A9: Rotemberg Weights by Industry

Industry	**Weight**	**Industry**	**Weight**
Services	0.000	Furniture	0.010
Metal Machinery	0.008	Vehicles Other	0.013
Agriculture	0.008	Mineral	0.017
Manufacturing, other	0.008	Metal Products	0.019
Metal Products	0.008	Machinery	0.023
Construction	0.009	Food	0.039
Agriculture	0.009	Petrochemicals	0.048
Mining	0.009	Metal Basic	0.081
Research	0.009	Electronics	0.084
Textiles	0.009	Manufact Other	0.122
Utilities	0.009	Automotive	0.448
Paper	0.009		

Table A10: Effect of robots on time use, adjusting for commuting-zone-specific trends across quartiles of employment share in the automotive sector (2SLS).

	Males			Females		
	(1)	(2)	(3)	(4)	(5)	(6)
Daily minutes work						
Robots	14.44**	10.29**	16.99**	-11.32**	-13.49**	-10.65
	(6.968)	(4.514)	(7.935)	(5.224)	(6.300)	(6.768)
Daily minutes childcare						
Robots	1.913	2.307	1.212	3.918	9.218***	9.417***
	(2.503)	(1.976)	(2.645)	(3.094)	(2.873)	(3.644)
Daily minutes leisure						
Robots	-9.457***	-5.544*	-12.87***	7.294**	9.601***	9.024**
	(3.413)	(3.277)	(3.969)	(3.565)	(3.524)	(4.149)
Spouse employed	✓		✓	✓		✓
Respondent employed		✓	✓		✓	✓

Notes: Controls include commuting zone and state-by-year FE, household controls, day/month/holiday. Sample: Individuals living with a spouse and children aged 10 or less. Standard errors clustered at the commuting-zone–year level. *** $p < 0.01$, ** $p < 0.05$, * $p < 0.1$.

Table A11: Effect of robots on time use (2SLS). Adão et al. (2019) test for standard errors.

	Males			Females		
	(1)	(2)	(3)	(4)	(5)	(6)
Daily minutes work						
Robots	13.92	8.38	18.02***	-15.40***	-18.91***	-15.26***
	(18.82)	(22.65)	(3.21)	(5.44)	(1.87)	(4.49)
Daily minutes childcare						
Robots	0.16	1.69	-0.77	6.61	8.22	8.45***
	(1.30)	(15.66)	(6.88)	(5.27)	(6.12)	(1.43)
Daily minutes leisure						
Robots	-8.79	-3.87	-11.87	6.75***	10.13***	9.41***
	(17.21)	(9.70)	(7.89)	(1.89)	(0.48)	(0.99)
Spouse employed	✓		✓	✓		✓
Respondent employed		✓	✓		✓	✓

Notes: Controls include commuting zone and state-by-year FE, household controls, day/month/holiday. Sample: Individuals living with a spouse and children aged 10 or less. Standard errors calculated using the Adão et al. (2019) procedure. *** $p < 0.01$, ** $p < 0.05$, * $p < 0.1$.

B Relative earnings and family beliefs

Additional stylized facts can be drawn from the *Family and Changing Gender Roles IV* module of the ISSP survey described in ISSP Research Group (2016). Respondents report their earnings relative to their spouse on a seven-point scale ranging from "My spouse/partner has no income" to "I have no income." Furthermore, they express agreement with a series of statements on family norms, such as "A preschool child is likely to suffer when the mother works" and "Family life suffers when a woman has a full-time job."[17]

Restricting the sample to U.S. couples and excluding the extreme tails of the earnings distribution,[18] I estimate the following specification:

$$\text{Belief}_i = \alpha + \sum_k \beta_k \, \mathbb{I}(\text{RelEarn}_i = k) + \mu X_i + \varepsilon_i, \tag{18}$$

where the dependent variable is the agreement score for a given family-norm statement (higher score indicates disagreement); $\mathbb{I}(\text{RelEarn}_i = k)$ is a vector of dummy variables indicating the wife's earnings position relative to her husband; and X_i controls for respondent sex, both spouses' ages and education levels, and marriage duration. Standard errors are clustered by respondent and spouse education. Appendix Figure A1 presents the resulting marginal-effects plots.

Across statements, a distinct non-monotonicity emerges. For items stressing the disadvantages of maternal employment or endorsing traditional spousal roles (Panels a–d), the disagreement score follows an inverse-U pattern. Respondents move from agreement (low score) when the wife earns far less, to strong disagreement (high score) near earnings parity, and then revert back toward agreement once the wife clearly out-earns the husband. This reversion suggests that couples in non-traditional earnings arrangements may ostensibly adopt more traditional attitudes to compensate for the deviation from the norm.

By contrast, attitudes toward maternal employment when children are older (Panel f) trace a U-shape in the disagreement score: couples at parity are the most likely to agree that women should work, while those with unequal earnings are more likely to disagree. Responses regarding maternal employment with preschool-age children (Panel e) display a similar but weaker downward trend, indicating less sensitivity to relative earnings for this specific issue.

[17] Two additional items—"Being a housewife is as fulfilling as working for pay" and "Both partners should contribute to household income"—were dropped because their directional interpretation regarding traditionalism is ambiguous.

[18] Including extreme points strengthens the observed dynamics but may confound the results with involuntary unemployment effects.

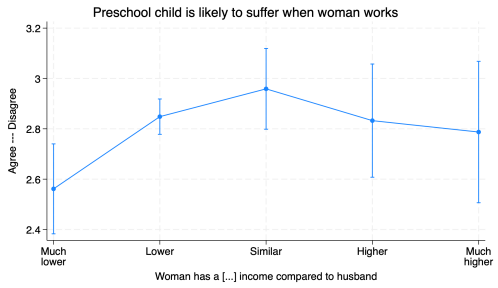

"Preschool child suffers if mother works"

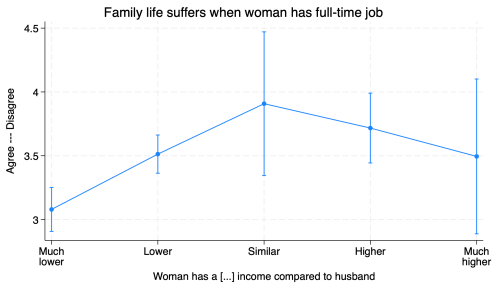

"Family life suffers if woman works full-time"

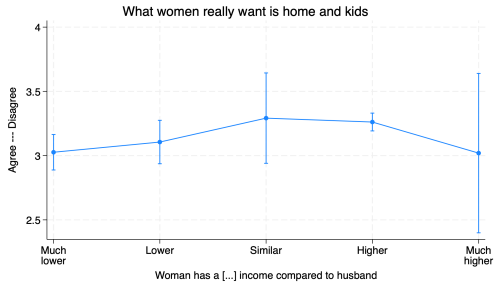

"What women really want is home/kids"

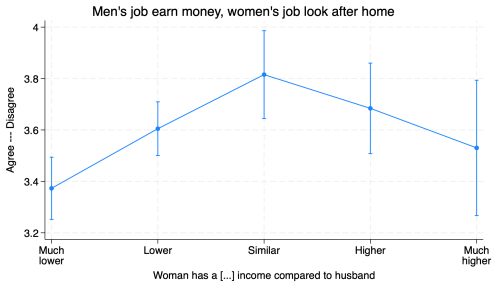

"Man's job is to earn money, woman's is home"

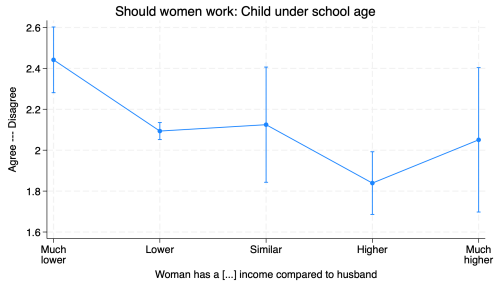

"Should women work: Child under school age"

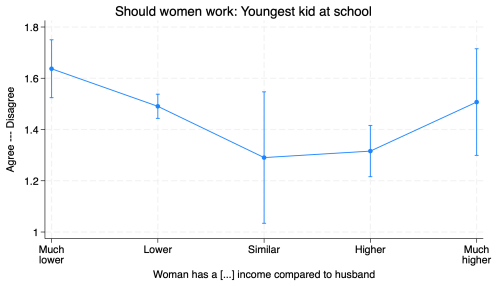

"Should women work: Youngest kid at school"

Figure A1: Marginal effects of the wife's relative earnings on agreement with family-norm statements. The y-axis represents the disagreement score (higher = less traditional). The x-axis represents the wife's contribution to household income, ranging from much less than the husband (left) to much more (right).

C Solution of the semi-cooperative model

The Lagrangian of the second stage problem is:

$$L_i = \delta_i \log\big(c\big) \;+\; \mu_i \log\big(1-(t_i+\tilde{t})\,n-h_i\big) \;+\; \gamma_i \log\big(n\,(1+t_i)^{\alpha}\,(1+t_{-i})^{1-\alpha}\big) \;+\; \eta\,t_i \;+\; \sigma\,t_{-i}$$

where η and σ are the Kuhn-Tucker multipliers associated to the non-negativity constraints on childcare time. The optimal solution satisfies $\eta t_f = \sigma t_m = 0$. The Nash Equilibrium of the second stage of the game can be in four regions, namely: $(\eta > 0, \sigma > 0), (\eta = 0, \sigma = 0), (\eta > 0, \sigma = 0), (\eta = 0, \sigma > 0)$.

The Lagrangian for the maximization of the first stage problem is

$$\begin{aligned} L = \theta\big(\delta_f \log(c) + \mu_f \log\big(1-(t_f+\tilde{t})\,n-h_f\big) + \gamma_f \log\big(n\,(1+t_f)^{\alpha}\,(1+t_m)^{1-\alpha}\big)\big) \\ +(1-\theta)\big(\delta_m \log(c) + \mu_m \log\big(1-(t_m+\tilde{t}m)\,n-h_m\big) \\ +\gamma_m \log\big(n\,(1+t_f)^{\alpha}\,(1+t_m)^{1-\alpha}\big)\big) + \tau\,h_f + \nu\,h_m, \end{aligned}$$

where τ and ν are the Kuhn-Tucker multipliers associated to the non-negativity constraints on working time. The optimal solution satisfies $\tau h_f = \nu h_m = 0$, with the exception of the case $h_f = h_m = 0$. We get three possible solutions for each of the four regions defined in the second stage, for a total of 12 possible time allocation regimes, listed below.

Regime 1a: $\eta > 0, \sigma > 0, \tau = 0, \nu = 0$

$$h_m = \frac{\begin{array}{l}\Big((\theta-1)nw_f + (1-\theta)\phi n\Big)\tilde{t}_f + (1-\theta)w_f + (\theta-1)\phi\Big)\,\mu_m \\ +\big(\theta n w_m \tilde{t}_m - \theta w_m\big)\,\mu_f \\ +\Big((1-\theta)nw_m\tilde{t}_m + (\theta-1)w_m\Big)\,\delta_m \\ +\big(\theta n w_m \tilde{t}_m - \theta w_m\big)\,\delta_f\end{array}}{(\theta-1)w_m\,\mu_m - \theta w_m\,\mu_f + (\theta-1)w_m\,\delta_m - \theta w_m\,\delta_f}$$

$$h_f = -\frac{\begin{array}{l}\Big((\theta-1)nw_f+(1-\theta)\phi n\Big)\tilde{t}_f+(1-\theta)w_f+(\theta-1)\phi\Big)\,\mu_m \\ +\left(\theta n w_m\tilde{t}_m-\theta w_m\right)\mu_f \\ +\Big((\theta-1)nw_f+(1-\theta)\phi n\Big)\tilde{t}_f+(1-\theta)w_f+(\theta-1)\phi\Big)\,\delta_m \\ +\Big((\theta\phi n-\theta n w_f)\tilde{t}_f+\theta w_f-\theta\phi\Big)\,\delta_f\end{array}}{\begin{array}{r}\Big((\theta-1)w_f+(1-\theta)\phi\Big)\mu_m+(\theta\phi-\theta w_f)\mu_f \\ +\Big((\theta-1)w_f+(1-\theta)\phi\Big)\delta_m+(\theta\phi-\theta w_f)\delta_f\end{array}}$$

$$t_m = 0$$

$$t_f = 0$$

Regime 1b: $\eta > 0, \sigma > 0, \tau = 0, \nu > 0$

$$h_m = 0$$

$$h_f = \frac{\left((\theta-1)n\tilde{t}_f-\theta+1\right)\delta_m+\left(\theta-\theta n\tilde{t}_f\right)\delta_f}{\theta\,\mu_f+(1-\theta)\delta_m+\theta\delta_f}$$

$$t_m = 0$$

$$t_f = 0$$

Regime 1c: $\eta > 0, \sigma > 0, \tau > 0, \nu = 0$

$$h_m = -\frac{\left((\theta-1)n\tilde{t}_m-\theta+1\right)\delta_m+\left(\theta-\theta n\tilde{t}_m\right)\delta_f}{(\theta-1)\mu_m+(\theta-1)\delta_m-\theta\delta_f}$$

$$h_f = 0$$

$$t_m = 0$$

$$t_f = 0$$

Regime 2a: $\eta = 0, \sigma = 0, \tau = 0, \nu = 0$

$$
\begin{aligned}
h_m = \frac{
&\Big((\theta-1)nw_f + (1-\theta)\phi n\Big)\tilde{t}_f + \big((1-\theta)n - \theta + 1\big)w_f + (\theta-1)\phi n + (\theta-1)\phi\Big)\,\mu_m \\
&+ \Big(\theta n w_m \tilde{t}_m + (-\theta n - \theta)w_m\Big)\,\mu_f \\
&+ \Big((1-\theta)n w_m \tilde{t}_m + \big((\theta-1)n + \theta - 1\big)w_m\Big)\,\delta_m \\
&+ \Big(\theta n w_m \tilde{t}_m + (-\theta n - \theta)w_m\Big)\,\delta_f \\
&+ \Big((\alpha - \alpha\theta)n w_m \tilde{t}_m + \big((1-\alpha)\theta + \alpha - 1\big)n w_f \tilde{t}_f + \big((\alpha-1)\theta - \alpha + 1\big)\phi n \tilde{t}_f \\
&\quad + (\alpha\theta - \alpha)n w_m + \big(((\alpha-1)\theta - \alpha + 1)n + (\alpha-1)\theta - \alpha + 1\big)w_f \\
&\quad + \big((1-\alpha)\theta + \alpha - 1\big)\phi n + \big((1-\alpha)\theta + \alpha - 1\big)\phi\Big)\gamma_m \\
&+ \Big(\alpha\theta n w_m \tilde{t}_m + \big((\alpha-1)\theta n w_f + (1-\alpha)\theta\phi n\big)\tilde{t}_f \\
&\quad + (-\alpha\theta n - \alpha\theta)w_m + \big((1-\alpha)\theta n + (1-\alpha)\theta\big)w_f + (\alpha-1)\theta\phi n + (\alpha-1)\theta\phi\Big)\gamma_f
\end{aligned}
}{
\begin{aligned}
&(\theta-1)w_m\,\mu_m - \theta w_m\,\mu_f + (\theta-1)w_m\,\delta_m - \theta w_m\,\delta_f \\
&\qquad + (\theta-1)w_m\,\gamma_m - \theta w_m\,\gamma_f
\end{aligned}
}
$$

$$
\begin{aligned}
h_f = -\frac{}{}
&\Big((\theta-1)nw_f+(1-\theta)\phi n\Big)\tilde{t}_f+\big((1-\theta)n-\theta+1\big)w_f+(\theta-1)\phi n+(\theta-1)\phi\Big)\,\mu_m\\
&+\Big(\theta n w_m\tilde{t}_m+(-\theta n-\theta)w_m\Big)\,\mu_f\\
&+\Big((\theta-1)nw_f+(1-\theta)\phi n\Big)\tilde{t}_f+\big((1-\theta)n-\theta+1\big)w_f+(\theta-1)\phi n+(\theta-1)\phi\Big)\,\delta_m\\
&+\Big((\theta\phi n-\theta n w_f)\tilde{t}_f+(\theta n+\theta)w_f-\theta\phi n-\theta\phi\Big)\,\delta_f\\
&+\Big((\alpha-\alpha\theta)nw_m\tilde{t}_m+\big((1-\alpha)\theta+\alpha-1\big)nw_f\tilde{t}_f+\big((\alpha-1)\theta-\alpha+1\big)\phi n\tilde{t}_f\\
&\quad+(\alpha\theta-\alpha)nw_m+\big(((\alpha-1)\theta-\alpha+1)n+(\alpha-1)\theta-\alpha+1\big)w_f\\
&\quad+\big((1-\alpha)\theta+\alpha-1\big)\phi n+\big((1-\alpha)\theta+\alpha-1\big)\phi\Big)\gamma_m\\
&+\Big(\alpha\theta n w_m\tilde{t}_m+\big((\alpha-1)\theta n w_f+(1-\alpha)\theta\phi n\big)\tilde{t}_f\\
&\quad+(-\alpha\theta n-\alpha\theta)w_m+\big((1-\alpha)\theta n+(1-\alpha)\theta\big)w_f+(\alpha-1)\theta\phi n+(\alpha-1)\theta\phi\Big)\gamma_f
\end{aligned}
$$

$$
\begin{aligned}
&\Big((\theta-1)w_f+(1-\theta)\phi\Big)\mu_m+(\theta\phi-\theta w_f)\mu_f\\
&\quad+\Big((\theta-1)w_f+(1-\theta)\phi\Big)\delta_m+(\theta\phi-\theta w_f)\delta_f\\
&\quad+\Big((\theta-1)w_f+(1-\theta)\phi\Big)\gamma_m+(\theta\phi-\theta w_f)\gamma_f
\end{aligned}
$$

$$
\begin{aligned}
t_m = -\frac{}{}
&(\theta-1)nw_m\,\mu_m^2 \\
&+\Big(-\theta nw_m\,\mu_f+(\theta-1)nw_m\,\delta_m-\theta nw_m\,\delta_f \\
&\quad+\Big(((1-\alpha)\theta+\alpha-1)nw_m\tilde{t}_m+((1-\alpha)\theta+\alpha-1)nw_f\tilde{t}_f \\
&\qquad+\big((\alpha-1)\theta-\alpha+1\big)\phi n\tilde{t}_f+\big((\theta-1)n+(\alpha-1)\theta-\alpha+1\big)w_m \\
&\qquad+\big(((\alpha-1)\theta-\alpha+1)n+(\alpha-1)\theta-\alpha+1\big)w_f \\
&\qquad+\big((1-\alpha)\theta+\alpha-1\big)\phi n+\big((1-\alpha)\theta+\alpha-1\big)\phi\Big)\gamma_m-\theta nw_m\,\gamma_f\Big)\mu_m \\
&+\alpha-1)\theta nw_m\,\gamma_m\,\mu_f \\
&+\big((1-\alpha)\theta+\alpha-1\big)nw_m\,\gamma_m\,\delta_m+(\alpha-1)\theta nw_m\,\gamma_m\,\delta_f \\
&+\Big(((\alpha^2-2\alpha+1)\theta-\alpha^2+2\alpha-1)nw_m\tilde{t}_m \\
&\quad+((\alpha^2-2\alpha+1)\theta-\alpha^2+2\alpha-1)nw_f\tilde{t}_f \\
&\quad+\big((-\alpha^2+2\alpha-1)\theta+\alpha^2-2\alpha+1\big)\phi n\tilde{t}_f \\
&\quad+\big(((\alpha-\alpha^2)\theta+\alpha^2-\alpha)n+(-\alpha^2+2\alpha-1)\theta+\alpha^2-2\alpha+1\big)w_m \\
&\quad+\big((-\alpha^2+2\alpha-1)\theta n+(-\alpha^2+2\alpha-1)\theta\big)w_f \\
&\quad+\big((\alpha^2-2\alpha+1)\theta-\alpha^2+2\alpha-1\big)\phi n+\big((\alpha^2-2\alpha+1)\theta-\alpha^2+2\alpha-1\big)\phi\Big)\gamma_m^2 \\
&+\Big((-\alpha^2+2\alpha-1)\theta nw_m\tilde{t}_m+\big((-\alpha^2+2\alpha-1)\theta nw_f+(\alpha^2-2\alpha+1)\theta\phi n\big)\tilde{t}_f \\
&\quad+\big((\alpha^2-\alpha)\theta n+(\alpha^2-2\alpha+1)\theta\big)w_m+\big((\alpha^2-2\alpha+1)\theta n+(\alpha^2-2\alpha+1)\theta\big)w_f \\
&\quad+(-\alpha^2+2\alpha-1)\theta\phi n+(-\alpha^2+2\alpha-1)\theta\phi\Big)\gamma_f\gamma_m \\
&\qquad\qquad (\theta-1)nw_m\,\mu_m^2 \\
&\qquad\qquad+\Big(-\theta nw_m\,\mu_f+(\theta-1)nw_m\,\delta_m-\theta nw_m\,\delta_f \\
&\qquad\qquad\quad+\big((2-2\alpha)\theta+2\alpha-2\big)nw_m\,\gamma_m-\theta nw_m\,\gamma_f\Big)\mu_m \\
&\qquad\qquad+\alpha-1)\theta nw_m\,\gamma_m\,\mu_f \\
&\qquad\qquad+\big((1-\alpha)\theta+\alpha-1\big)nw_m\,\gamma_m\,\delta_m+(\alpha-1)\theta nw_m\,\gamma_m\,\delta_f \\
&\qquad\qquad+\big((\alpha^2-2\alpha+1)\theta-\alpha^2+2\alpha-1\big)nw_m\,\gamma_m^2 \\
&\qquad\qquad+\big(-\alpha^2+2\alpha-1\big)\theta nw_m\,\gamma_f\gamma_m
\end{aligned}
$$

$$
t_f = -\frac{\begin{array}{l}\big((\theta-1)nw_f+(1-\theta)\phi n\big)\mu_f\,\mu_m+\big((\alpha\theta-\alpha)nw_f+(\alpha-\alpha\theta)\phi n\big)\gamma_f\mu_m\\ +\big(\theta\phi n-\theta nw_f\big)\mu_f^2\\ +\big((\theta-1)nw_f+(1-\theta)\phi n\big)\delta_m+\big(\theta\phi n-\theta nw_f\big)\delta_f\\ +\big((\alpha\theta-\alpha)nw_f+(\alpha-\alpha\theta)\phi n\big)\gamma_m\\ +\Big(-\alpha\theta nw_m\tilde{t}_m+(\alpha\theta\phi n-\alpha\theta nw_f)\tilde{t}_f+\alpha\theta w_m+(\alpha\theta-\alpha\theta n)w_f+\alpha\theta\phi n-\alpha\theta\phi\Big)\gamma_f\\ +\big((\alpha\theta-\alpha)nw_f+(\alpha-\alpha\theta)\phi n\big)\gamma_f\delta_m+\big(\alpha\theta\phi n-\alpha\theta nw_f\big)\gamma_f\delta_f\\ +\Big((\alpha^2\theta-\alpha^2)nw_m\tilde{t}_m+\big((\alpha^2\theta-\alpha^2)nw_f\\ +(\alpha^2-\alpha^2\theta)\phi n\big)\tilde{t}_f+(\alpha^2-\alpha^2\theta)(w_m+w_f)+(\alpha^2\theta-\alpha^2)\phi\Big)\gamma_f\gamma_m\\ +\Big(-\alpha^2\theta nw_m\tilde{t}_m+(\alpha^2\theta\phi n-\alpha^2\theta nw_f)\tilde{t}_f+\alpha^2\theta(w_m+w_f)-\alpha^2\theta\phi\Big)\gamma_f^2\end{array}}{\begin{array}{l}\big((\theta-1)nw_f+(1-\theta)\phi n\big)\mu_f\,\mu_m+\big((\alpha\theta-\alpha)nw_f+(\alpha-\alpha\theta)\phi n\big)\gamma_f\mu_m\\ +\big(\theta\phi n-\theta nw_f\big)\mu_f^2\\ +\big((\theta-1)nw_f+(1-\theta)\phi n\big)\delta_m+\big(\theta\phi n-\theta nw_f\big)\delta_f\\ +\big((\alpha\theta-\alpha)nw_f+(\alpha-\alpha\theta)\phi n\big)\gamma_m\\ +\big(2\alpha\theta\phi n-2\alpha\theta nw_f\big)\gamma_f\\ +\big((\alpha\theta-\alpha)nw_f+(\alpha-\alpha\theta)\phi n\big)\gamma_f\delta_m+\big(\alpha\theta\phi n-\alpha\theta nw_f\big)\gamma_f\delta_f\\ +\big((\alpha\theta-\alpha)nw_f+(\alpha-\alpha\theta)\phi n\big)\gamma_f\gamma_m+\big(\alpha\theta\phi n-\alpha\theta nw_f\big)\gamma_f^2\end{array}}
$$

Regime 2b: $\eta = 0, \sigma = 0, \tau = 0, \nu > 0$

$$
h_m = 0
$$

$$
h_f = \frac{\big((\theta-1)n\tilde{t}_f+(1-\theta)n-\theta+1\big)\,\delta_m+\big(-\theta n\tilde{t}_f+\theta n+\theta\big)\,\delta_f}{\theta\,\mu_f+(1-\theta)\delta_m+\theta\delta_f+(\alpha-\alpha\theta)\gamma_m+\alpha\theta\gamma_f}
$$

$$
t_m = -\frac{n\,\mu_m+\big((1-\alpha)n\tilde{t}_m+\alpha-1\big)\gamma_m}{n\,\mu_m+(1-\alpha)n\,\gamma_m}
$$

$$
t_f = -\frac{\begin{array}{l}\theta n\,\mu_f^2 \\ \quad + \Big((1-\theta)n\,\delta_m + \theta n\,\delta_f + (\alpha-\alpha\theta)n\,\gamma_m + (\alpha\theta n\tilde{t}_f + \alpha\theta n - \alpha\theta)\gamma_f\Big)\mu_f \\ \quad + \big(\alpha-\alpha\theta\big)n\,\gamma_f\,\delta_m + \alpha\theta n\,\gamma_f\,\delta_f \\ \quad + \Big((\alpha^2-\alpha^2\theta)n\tilde{t}_f + \alpha^2\theta - \alpha^2\Big)\gamma_f\gamma_m + \big(\alpha^2\theta n\tilde{t}_f - \alpha^2\theta\big)\gamma_f^2\end{array}}{\begin{array}{l}\theta n\,\mu_f^2 \\ \quad + \Big((1-\theta)n\,\delta_m + \theta n\,\delta_f + (\alpha-\alpha\theta)n\,\gamma_m + 2\alpha\theta n\,\gamma_f\Big)\mu_f \\ \quad + \big(\alpha-\alpha\theta\big)n\,\gamma_f\,\delta_m + \alpha\theta n\,\gamma_f\,\delta_f \\ \quad + \big(\alpha^2-\alpha^2\theta\big)n\,\gamma_f\gamma_m + \alpha^2\theta n\,\gamma_f^2\end{array}}
$$

Regime 2c: $\eta = 0, \sigma = 0, \tau > 0, \nu = 0$

$$
h_m = -\frac{\big((\theta-1)n\tilde{t}_m + (1-\theta)n - \theta + 1\big)\,\delta_m + \big(-\theta n\tilde{t}_m + \theta n + \theta\big)\,\delta_f}{(\theta-1)\mu_m + (\theta-1)\delta_m - \theta\delta_f + ((1-\alpha)\theta + \alpha - 1)\gamma_m + (\alpha-1)\theta\gamma_f}
$$

$$
h_f = 0
$$

$$
t_m = -\frac{\begin{array}{l}(\theta-1)n\,\mu_m^2 \\ \quad + \Big((\theta-1)n\,\delta_m - \theta n\,\delta_f + \big(((1-\alpha)\theta + \alpha - 1)n\tilde{t}_m \\ \quad + ((1-\alpha)\theta + \alpha - 1)n + (\alpha-1)\theta - \alpha + 1\big)\gamma_m \quad + (\alpha-1)\theta n\,\gamma_f\Big)\mu_m \\ \quad + \big((1-\alpha)\theta + \alpha - 1\big)n\gamma_m\,\delta_m + (\alpha-1)\theta n\gamma_m\,\delta_f \\ \quad + \Big(((\alpha^2-2\alpha+1)\theta - \alpha^2 + 2\alpha - 1)n\tilde{t}_m + (-\alpha^2+2\alpha-1)\theta + \alpha^2 - 2\alpha + 1\Big)\gamma_m^2 \\ \quad + \Big((-\alpha^2+2\alpha-1)\theta n\tilde{t}_m + (\alpha^2-2\alpha+1)\theta\Big)\gamma_f\gamma_m\end{array}}{\begin{array}{l}(\theta-1)n\,\mu_m^2 \\ \quad + \Big((\theta-1)n\,\delta_m - \theta n\,\delta_f + \big((2-2\alpha)\theta + 2\alpha - 2\big)n\gamma_m + (\alpha-1)\theta n\,\gamma_f\Big)\mu_m \\ \quad + \big((1-\alpha)\theta + \alpha - 1\big)n\gamma_m\,\delta_m + (\alpha-1)\theta n\gamma_m\,\delta_f \\ \quad + \big((\alpha^2-2\alpha+1)\theta - \alpha^2 + 2\alpha - 1\big)n\gamma_m^2 + (-\alpha^2+2\alpha-1)\theta n\,\gamma_f\gamma_m\end{array}}
$$

$$
t_f = -\frac{n\,\mu_f + (\alpha n\tilde{t}_f - \alpha)\gamma_f}{n\,\mu_f + \alpha n\,\gamma_f}
$$

Regime 3a: $\eta > 0, \sigma = 0, \tau = 0, \nu = 0$

$$h_m = \frac{\begin{array}{l}\Big((\theta-1)nw_f + (1-\theta)\phi n\Big)\tilde{t}_f + (1-\theta)w_f + (\theta-1)\phi\Big)\,\mu_m \\ + \Big(\theta n w_m \tilde{t}_m + (-\theta n - \theta)w_m\Big)\,\mu_f \\ + \Big((1-\theta)nw_m\tilde{t}_m + \big((\theta-1)n + \theta - 1\big)w_m\Big)\,\delta_m \\ + \Big(\theta n w_m \tilde{t}_m + (-\theta n - \theta)w_m\Big)\,\delta_f \\ + \Big(\big((1-\alpha)\theta + \alpha - 1\big)nw_f + \big((\alpha-1)\theta - \alpha + 1\big)\phi n\Big)\tilde{t}_f \\ + \big((\alpha-1)\theta - \alpha + 1\big)w_f + \big((1-\alpha)\theta + \alpha - 1\big)\phi\Big)\,\gamma_m \\ + \Big(\big((\alpha-1)\theta n w_f + (1-\alpha)\theta\phi n\big)\tilde{t}_f + (1-\alpha)\theta w_f + (\alpha-1)\theta\phi\Big)\,\gamma_f\end{array}}{\begin{array}{l}(\theta-1)w_m\,\mu_m - \theta w_m\,\mu_f \\ + \big((\theta-1)w_m - \theta w_m\big)\delta_m - \theta w_m\,\delta_f \\ + \big((1-\alpha)\theta + \alpha - 1\big)w_m\,\gamma_m + (\alpha-1)\theta w_m\,\gamma_f\end{array}}$$

$$h_f = -\frac{\begin{array}{l}\Big((\theta-1)nw_f + (1-\theta)\phi n\Big)\tilde{t}_f + (1-\theta)w_f + (\theta-1)\phi\Big)\,\mu_m \\ + \Big(\theta n w_m \tilde{t}_m + (-\theta n - \theta)w_m\Big)\,\mu_f \\ + \Big((\theta-1)nw_f + (1-\theta)\phi n\Big)\tilde{t}_f + (1-\theta)w_f + (\theta-1)\phi\Big)\,\delta_m \\ + \Big((\theta\phi n - \theta n w_f)\tilde{t}_f + \theta w_f - \theta\phi\Big)\,\delta_f \\ + \Big(\big((1-\alpha)\theta + \alpha - 1\big)nw_f + \big((\alpha-1)\theta - \alpha + 1\big)\phi n\Big)\tilde{t}_f + \big((\alpha-1)\theta - \alpha + 1\big)w_f + \big((1-\alpha)\theta \\ + \alpha - 1\big)\phi\Big)\,\gamma_m + \Big(\big((\alpha-1)\theta n w_f + (1-\alpha)\theta\phi n\big)\tilde{t}_f + (1-\alpha)\theta w_f + (\alpha-1)\theta\phi\Big)\,\gamma_f\end{array}}{\begin{array}{l}\Big((\theta-1)w_f + (1-\theta)\phi\Big)\mu_m + (\theta\phi - \theta w_f)\mu_f \\ + \Big((\theta-1)w_f + (1-\theta)\phi\Big)\delta_m + (\theta\phi - \theta w_f)\delta_f \\ + \big((1-\alpha)\theta + \alpha - 1\big)w_f + \big((\alpha-1)\theta - \alpha + 1\big)\phi\Big)\gamma_m \\ + \big((\alpha-1)\theta w_f + (1-\alpha)\theta\phi\big)\gamma_f\end{array}}$$

$$
\begin{aligned}
t_m = -\ & \frac{(\theta-1)nw_m\,\mu_m^2} \\
& + \Big(-\theta nw_m\,\mu_f + (\theta-1)nw_m\,\delta_m - \theta nw_m\,\delta_f \\
& \quad + \Big(((1-\alpha)\theta+\alpha-1)nw_m\tilde{t}_m + ((1-\alpha)\theta+\alpha-1)nw_f\tilde{t}_f \\
& \qquad + \big((\alpha-1)\theta-\alpha+1\big)\phi n\tilde{t}_f + \big(((1-\theta)+\alpha-1)n + (\alpha-1)\theta-\alpha+1\big)w_m \\
& \qquad + \big((\alpha-1)\theta-\alpha+1\big)w_f + \big((1-\alpha)\theta+\alpha-1\big)\phi\Big)\gamma_m + (\alpha-1)\theta nw_m\,\gamma_f\Big)\mu_m \\
& + \big(\alpha-1\big)\theta nw_m\,\gamma_m\,\mu_f \\
& + \big((1-\alpha)\theta+\alpha-1\big)nw_m\,\gamma_m\,\delta_m + (\alpha-1)\theta nw_m\,\gamma_m\,\delta_f \\
& + \Big(((\alpha^2-2\alpha+1)\theta-\alpha^2+2\alpha-1)nw_m\tilde{t}_m \\
& \quad + ((\alpha^2-2\alpha+1)\theta-\alpha^2+2\alpha-1)nw_f\tilde{t}_f \\
& \quad + \big((-\alpha^2+2\alpha-1)\theta+\alpha^2-2\alpha+1\big)\phi n\tilde{t}_f \\
& \quad + \big((-\alpha^2+2\alpha-1)\theta+\alpha^2-2\alpha+1\big)w_m \\
& \quad + \big((-\alpha^2+2\alpha-1)\theta+\alpha^2-2\alpha+1\big)w_f \\
& \quad + \big((\alpha^2-2\alpha+1)\theta-\alpha^2+2\alpha-1\big)\phi\Big)\gamma_m^2 \\
& + \Big((-\alpha^2+2\alpha-1)\theta nw_m\tilde{t}_m + \big((-\alpha^2+2\alpha-1)\theta nw_f + (\alpha^2-2\alpha+1)\theta\phi n\big)\tilde{t}_f \\
& \quad + \big((\alpha^2-2\alpha+1)\theta+\alpha^2-2\alpha+1\big)w_m \\
& \quad + \big((\alpha^2-2\alpha+1)\theta+\alpha^2-2\alpha+1\big)w_f + (-\alpha^2+2\alpha-1)\theta\phi\Big)\gamma_f\gamma_m \\
& \hline \\
& (\theta-1)nw_m\,\mu_m^2 \\
& \quad + \Big(-\theta nw_m\,\mu_f + (\theta-1)nw_m\,\delta_m - \theta nw_m\,\delta_f \\
& \qquad + \big((2-2\alpha)\theta+2\alpha-2\big)nw_m\,\gamma_m + (\alpha-1)\theta nw_m\,\gamma_f\Big)\mu_m \\
& \quad + \big(\alpha-1\big)\theta nw_m\,\gamma_m\,\mu_f \\
& \quad + \big((1-\alpha)\theta+\alpha-1\big)nw_m\,\gamma_m\,\delta_m + (\alpha-1)\theta nw_m\,\gamma_m\,\delta_f \\
& \quad + \big((\alpha^2-2\alpha+1)\theta-\alpha^2+2\alpha-1\big)nw_m\,\gamma_m^2 + (-\alpha^2+2\alpha-1)\theta nw_m\,\gamma_f\gamma_m
\end{aligned}
$$

$$
t_f = 0
$$

Regime 3b: $\eta > 0, \sigma = 0, \tau = 0, \nu > 0$

$$h_m = 0$$

$$h_f = \frac{\big((\theta-1)n\tilde{t}_f - \theta + 1\big)\,\delta_m + \big(\theta - \theta n\tilde{t}_f\big)\,\delta_f}{\theta\,\mu_f + (1-\theta)\delta_m + \theta\delta_f}$$

$$t_m = -\,\frac{n\,\mu_m + \big((1-\alpha)n\tilde{t}_m + \alpha - 1\big)\gamma_m}{n\,\mu_m + (1-\alpha)n\,\gamma_m}$$

Regime 3c: $\eta > 0, \sigma = 0, \tau > 0, \nu = 0$

$$h_m = -\,\frac{\big((\theta-1)n\tilde{t}_m + (1-\theta)n - \theta + 1\big)\,\delta_m + \big(-\theta n\tilde{t}_m + \theta n + \theta\big)\,\delta_f}{(\theta-1)\mu_m + (\theta-1)\delta_m - \theta\delta_f + \big((1-\alpha)\theta + \alpha - 1\big)\gamma_m + (\alpha-1)\theta\gamma_f}$$

$$h_f = 0$$

$$t_m = -\,\frac{\begin{array}{l}(\theta-1)n\,\mu_m^2 \\ \quad + \Big((\theta-1)n\,\delta_m - \theta n\,\delta_f + \big((1-\alpha)\theta + \alpha - 1\big)n\tilde{t}_m + \big((1-\alpha)\theta + \alpha - 1\big)n \\ \qquad + (\alpha-1)\theta - \alpha + 1\Big)\gamma_m + (\alpha-1)\theta n\,\gamma_f\Big)\mu_m \\ \quad + \big((1-\alpha)\theta + \alpha - 1\big)n\gamma_m\,\delta_m + (\alpha-1)\theta n\gamma_m\,\delta_f \\ \quad + \big((\alpha^2 - 2\alpha + 1)\theta - \alpha^2 + 2\alpha - 1\big)n\tilde{t}_m + \big(-\alpha^2 + 2\alpha - 1\big)\theta + \alpha^2 - 2\alpha + 1\Big)\gamma_m^2 \\ \quad + \Big((-\alpha^2 + 2\alpha - 1)\theta n\tilde{t}_m + (\alpha^2 - 2\alpha + 1)\theta\Big)\gamma_f\gamma_m\end{array}}{\begin{array}{l}(\theta-1)n\,\mu_m^2 \\ \quad + \Big((\theta-1)n\,\delta_m - \theta n\,\delta_f + \big((2-2\alpha)\theta + 2\alpha - 2\big)n\gamma_m + (\alpha-1)\theta n\,\gamma_f\Big)\mu_m \\ \quad + \big((1-\alpha)\theta + \alpha - 1\big)n\gamma_m\,\delta_m + (\alpha-1)\theta n\gamma_m\,\delta_f \\ \quad + \big((\alpha^2 - 2\alpha + 1)\theta - \alpha^2 + 2\alpha - 1\big)n\gamma_m^2 + \big(-\alpha^2 + 2\alpha - 1\big)\theta n\,\gamma_f\gamma_m\end{array}}$$

$$t_f = 0$$

Regime 4a: $\eta = 0, \sigma > 0, \tau = 0, \nu = 0$

$$h_m = \frac{\begin{array}{l}\Big((\theta-1)nw_f + (1-\theta)\phi n\Big)\tilde{t}_f + \big((1-\theta)n - \theta + 1\big)w_f + (\theta-1)\phi n + (\theta-1)\phi\Big)\,\mu_m \\ + \big(\theta n w_m \tilde{t}_m - \theta w_m\big)\,\mu_f \\ + \Big((1-\theta)n w_m \tilde{t}_m + (\theta-1)w_m\Big)\,\delta_m \\ + \big(\theta n w_m \tilde{t}_m - \theta w_m\big)\,\delta_f \\ + \Big((\alpha - \alpha\theta)n w_m \tilde{t}_m + (\alpha\theta - \alpha)w_m\Big)\,\gamma_m \\ + \Big(\alpha\theta n w_m \tilde{t}_m - \alpha\theta w_m\Big)\,\gamma_f\end{array}}{\begin{array}{r}(\theta-1)w_m\,\mu_m - \theta w_m\,\mu_f + (\theta-1)w_m\,\delta_m - \theta w_m\,\delta_f \\ +(\alpha\theta - \alpha)w_m\,\gamma_m - \alpha\theta w_m\,\gamma_f\end{array}}$$

$$h_f = -\frac{\begin{array}{l}\Big((\theta-1)nw_f + (1-\theta)\phi n\Big)\tilde{t}_f + \big((1-\theta)n - \theta + 1\big)w_f + (\theta-1)\phi n + (\theta-1)\phi\Big)\,\mu_m \\ + \big(\theta n w_m \tilde{t}_m - \theta w_m\big)\,\mu_f \\ + \Big((\theta-1)nw_f + (1-\theta)\phi n\Big)\tilde{t}_f + \big((1-\theta)n - \theta + 1\big)w_f + (\theta-1)\phi n + (\theta-1)\phi\Big)\,\delta_m \\ + \Big((\theta\phi n - \theta n w_f)\tilde{t}_f + (\theta n + \theta)w_f - \theta\phi n - \theta\phi\Big)\,\delta_f \\ + \Big((\alpha - \alpha\theta)n w_m \tilde{t}_m + (\alpha\theta - \alpha)w_m\Big)\,\gamma_m \\ + \Big(\alpha\theta n w_m \tilde{t}_m - \alpha\theta w_m\Big)\,\gamma_f\end{array}}{\begin{array}{r}\Big((\theta-1)w_f + (1-\theta)\phi\Big)\mu_m + (\theta\phi - \theta w_f)\mu_f \\ + \Big((\theta-1)w_f + (1-\theta)\phi\Big)\delta_m + (\theta\phi - \theta w_f)\delta_f \\ + \Big((\alpha\theta - \alpha)w_f + (\alpha - \alpha\theta)\phi\Big)\gamma_m + (\alpha\theta\phi - \alpha\theta w_f)\gamma_f\end{array}}$$

$$t_m = 0$$

$$
t_f = -\frac{\begin{array}{l}
\Big((\theta-1)nw_f+(1-\theta)\phi n\Big)\mu_f+\Big((\alpha\theta-\alpha)nw_f+(\alpha-\alpha\theta)\phi n\Big)\gamma_f\Big)\mu_m \\
+\big(\theta\phi n-\theta nw_f\big)\mu_f^2 \\
+\Big((\theta-1)nw_f+(1-\theta)\phi n\Big)\delta_m+\big(\theta\phi n-\theta nw_f\big)\delta_f \\
+\Big((\theta-1)nw_f+(1-\theta)\phi n\Big)\gamma_m \\
+\Big(-\alpha\theta nw_m\tilde{t}_m+(\alpha\theta\phi n-\alpha\theta nw_f)\tilde{t}_f+(\alpha\theta n+\alpha\theta)w_m+(\alpha\theta-\theta n)w_f+\theta\phi n-\alpha\theta\phi\Big)\gamma_f \\
+\big((\alpha\theta-\alpha)nw_f+(\alpha-\alpha\theta)\phi n\big)\gamma_f\delta_m+\big(\alpha\theta\phi n-\alpha\theta nw_f\big)\gamma_f\delta_f \\
+\Big((\alpha^2\theta-\alpha^2)nw_m\tilde{t}_m+\big((\alpha^2\theta-\alpha^2)nw_f \\
+(\alpha^2-\alpha^2\theta)\phi n\big)\tilde{t}_f+(\alpha^2-\alpha^2\theta)(w_m+w_f)+(\alpha^2\theta-\alpha^2)\phi\Big)\gamma_f\gamma_m \\
+\Big(-\alpha^2\theta nw_m\tilde{t}_m+(\alpha^2\theta\phi n-\alpha^2\theta nw_f)\tilde{t}_f+\alpha^2\theta(w_m+w_f)-\alpha^2\theta\phi\Big)\gamma_f^2
\end{array}}{\begin{array}{l}
\Big((\theta-1)nw_f+(1-\theta)\phi n\Big)\mu_f+\Big((\alpha\theta-\alpha)nw_f+(\alpha-\alpha\theta)\phi n\Big)\gamma_f\Big)\mu_m \\
+\big(\theta\phi n-\theta nw_f\big)\mu_f^2 \\
+\Big((\theta-1)nw_f+(1-\theta)\phi n\Big)\delta_m+\big(\theta\phi n-\theta nw_f\big)\delta_f \\
+\Big((\theta-1)nw_f+(1-\theta)\phi n\Big)\gamma_m \\
+\big((-\alpha-1)\theta nw_f+(\alpha+1)\theta\phi n\big)\gamma_f\,\mu_f \\
+\big((\alpha\theta-\alpha)nw_f+(\alpha-\alpha\theta)\phi n\big)\gamma_f\delta_m+\big(\alpha\theta\phi n-\alpha\theta nw_f\big)\gamma_f\delta_f \\
+\big((\alpha\theta-\alpha)nw_f+(\alpha-\alpha\theta)\phi n\big)\gamma_f\gamma_m+\big(\alpha\theta\phi n-\alpha\theta nw_f\big)\gamma_f^2
\end{array}}
$$

Regime 4b: $\eta = 0, \sigma > 0, \tau = 0, \nu > 0$

$$h_m = 0$$

$$h_f = \frac{\big((\theta-1)n\tilde{t}_f+(1-\theta)n-\theta+1\big)\,\delta_m+\big(-\theta n\tilde{t}_f+\theta n+\theta\big)\,\delta_f}{\theta\,\mu_f+(1-\theta)\delta_m+\theta\delta_f+(\alpha-\alpha\theta)\gamma_m+\alpha\theta\gamma_f}$$

$$t_m = 0$$

$$
t_f = -\frac{\begin{aligned}
&\theta n\,\mu_f^2 + \Big((1-\theta)n\,\delta_m + \theta n\,\delta_f + (\alpha-\alpha\theta)n\,\gamma_m + (\alpha\theta n\tilde{t}_f + \alpha\theta n - \alpha\theta)\gamma_f\Big)\mu_f \\
&+ \big(\alpha-\alpha\theta\big)n\,\gamma_f\,\delta_m + \alpha\theta n\,\gamma_f\,\delta_f \\
&+ \Big((\alpha^2-\alpha^2\theta)n\tilde{t}_f + \alpha^2\theta - \alpha^2\Big)\gamma_f\gamma_m + \big(\alpha^2\theta n\tilde{t}_f - \alpha^2\theta\big)\gamma_f^2
\end{aligned}}{\begin{aligned}
&\theta n\,\mu_f^2 + \Big((1-\theta)n\,\delta_m + \theta n\,\delta_f + (\alpha-\alpha\theta)n\,\gamma_m + 2\alpha\theta n\,\gamma_f\Big)\mu_f \\
&+ \big(\alpha-\alpha\theta\big)n\,\gamma_f\,\delta_m + \alpha\theta n\,\gamma_f\,\delta_f \\
&+ \big(\alpha^2-\alpha^2\theta\big)n\,\gamma_f\gamma_m + \alpha^2\theta n\,\gamma_f^2
\end{aligned}}
$$

Regime 4c: $\eta = 0, \sigma > 0, \tau > 0, \nu = 0$

$$
h_m = -\frac{\big((\theta-1)n\tilde{t}_m - \theta + 1\big)\,\delta_m + \big(\theta - \theta n\tilde{t}_m\big)\,\delta_f}{(\theta-1)\mu_m + (\theta-1)\delta_m - \theta\delta_f}
$$

$$
h_f = 0
$$

$$
t_m = 0
$$

$$
t_f = -\frac{n\,\mu_f + (\alpha n\tilde{t}_f - \alpha)\gamma_f}{n\,\mu_f + \alpha n\,\gamma_f}
$$

C.1 Proof of Proposition 1

Stage 2. Fix (h_f, h_m). Player i solves a strictly concave problem in t_i:

$$
v_i(t_i; t_{-i}, h_f, h_m) = \log(c) + \mu_i \log\big(1 - h_i - (t_i + \tilde{t}_i)n\big) + \gamma_i \log\big((1+t_f)^{\alpha}(1+t_m)^{1-\alpha}n\big),
$$

over a nonempty, convex, compact interval for t_i (A3). The second derivative in own strategy,

$$
\frac{\partial^2 v_i}{\partial t_i^2} = -\frac{\mu_i n^2}{\big(1 - h_i - (t_i + \tilde{t}_i)n\big)^2} - \frac{\gamma_i}{(1+t_i)^2} \times \begin{cases} \alpha & \text{if } i = f, \\ 1-\alpha & \text{if } i = m, \end{cases}
$$

is strictly negative, so each payoff is strictly concave in own action. The Jacobian of first-order conditions has a symmetric part whose diagonal entries dominate the off-diagonal terms (the cross–partial from $\log q$), implying diagonal strict concavity (DSC). By Rosen's (1965) theorem, a unique Nash equilibrium (t_f^*, t_m^*) exists; by the implicit function theorem and DSC, (t_f^*, t_m^*) is continuous in (h_f, h_m).

Stage 1. Define $V(h_f, h_m) = \theta v_f\big(h_f, h_m, t^*(h)\big) + (1-\theta) v_m\big(h_f, h_m, t^*(h)\big)$. The feasible set for (h_f, h_m) is convex/compact (A3). The only non-affine term in (h_f, h_m) is $\log c$ with $c = \phi(s) w_f h_f + w_m h_m$. Under A2, the mapping $(h_f, h_m) \mapsto \log c$ is strictly concave on the feasible set.[19] All remaining terms in V are (strictly) concave in (h_f, h_m), and composition with the single-valued continuous correspondence $t^*(h)$ preserves concavity. Hence V is strictly concave and attains a unique maximizer (h_f^*, h_m^*). Combining with the unique (t_f^*, t_m^*) from Stage 2 yields a unique subgame-perfect equilibrium.

□

[19] For $\phi(s) = \exp[-\chi s^\kappa]$ with $s = \frac{w_f h_f}{w_f h_f + w_m h_m}$ the Hessian of $\log c$ is negative definite whenever $\chi \leq \bar{\chi}(\kappa, w_f, w_m, \underline{h}, \overline{h})$; an explicit bound is obtained by comparing $|\partial^2 \log c / \partial h_i \partial h_j|$ with the diagonal terms and using the fact that $h_i \in [\underline{h}, \overline{h}]$. If s is defined on *potential* shares $w_f/(w_f + w_m)$, $\log c$ is strictly concave without any restriction on χ.